The Society of Naval Architects of Japan

(昭和十三年四月三日造船協會、造船協會阪神倶樂部聯合大會に於て講演)

Model Experiments of the Combined Effect of Breadth of Hull and Propeller Revolutions upon the Propulsive Economy of Single-Screw Ships.

By **Masao Yamagata,** *Kogakuhakusi, Member.*
The Teishinsho Ship Experiment Tank, Tokyo.

Introduction.

Research work on the combined effect of hull forms and propeller revolutions upon the propulsive economy of single-screw ships has been carried out at the Teishinsho Ship Experiment Tank in Tokyo during the last five years, and I have already published two papers,[1][2] giving the results of the experiments of the combined effect of after body forms and propeller revolutions upon the propulsive performance of moderate-speed cargo ships. The present paper is an account of the experiments, which were made as a part of this research work, with the object of investigating the optimum breadths of single-screw cargo liners of constant displacement and draught in conjunction with the propeller revolutions.

Ship Models Employed.

The experiments were made on four ship models, i. e., Nos. 237, 312, 313 and 314, which represented 137·158 metre single-screw cargo liners with cruiser sterns, intended to run at over 16 knots, when fully loaded. They were made to a scale of 1:22·860 in paraffin wax, and the leading particulars of the models were as follows:—

Model No.	312	237	313	314
Length pp. in m., L	6·0000	6·0000	6·0000	6·0000
Breadth ext. in m., B	0·7751	0·8151	0·8551	0·8951
Load draught in m., T	0·3617	0·3644	0·3637	0·3637
Load displt. in kg., Δ	1,217·6	1,217·6	1,217·6	1,217·6
Block coefft., δ	0·720	0·683	0·653	0·623
Prismatic coefft., φ	0·726	0·691	0·666	0·644
Midship coefft., β	0·992	0·988	0·980	0·968
Long. C.B. from ⊠ in m.	0·034 abaft	0·031 abaft	0·031 abaft	0·032 abaft

(1) Trans. Inst. N. A., Vol. 76 (1934), p. 387.
(2) Jour. Soc. N. A. Japan, No. 57 (Dec. 1935), p. 149.

NII-Electronic Library Service

The Society of Naval Architects of Japan

The sectional area curves are given in Fig. 1. The models were fitted with all appendages, and their body-plans, together with bow and stern arrangements, are shown in Figs. 2 to 5.

Resistance Tests.

Each of the ship models without and with appendages was run in smooth water on level trim at the load displacement to ascertain its resistance. In Figs. 6 to 9 the results are plotted in our standard non-dimensional form, and in Figs. 10 to 13 the effective horse-power curves of full-sized ships, calculated from the results shown in Figs. 6 to 9 by Froude's skin friction constants corrected to the standard temperature of 15°C. to correspond to clean-ship conditions in salt water without any allowance for air and wave resistances, are given on bases of speed in knots. In order to easily see the breadths of minimum resistance at various speeds, in Fig. 14 the effective horse-power curves for 15, 16, 17 and 18 knots are shown on a base of the ratio of breadth to length of hull, with an optimum breadth line. Since a broader ship is generally subjected to greater air resistance than a narrow one, it seems to be necessary to consider an air resistance for discussing the optimum breadth of hull. In general, an air resistance R_a can be approximately expressed by an equation of the form $R_a=c\frac{1}{2}\rho A V_a^2$, c being a numerical constant, ρ the density of air, A the transverse projected area of the above water portions of a ship, and V_a the relative wind velocity. Taking, for example, $c=1$ and $A=18B$ m^2., the air resistances in still air, i.e. at $V_a=V$, and in the head wind equal to ship's speed, i. e. at $V_a=2V$, were calculated, and added to the effective horse-powers deduced from the results of resistance tests, which could be considered as those at $V_a=0$. In Fig. 14 these two sets of effective horse-power curves are also given, with optimum breadth lines. It will be seen from this figure that, when the speed of a ship is under 16 knots, there is no distinct difference between the optimum breadths for various wind velocities, though, strictly speaking, the optimum breadth, of course, becomes smaller with the increase of relative wind velocity. For comparison, the similar test results[3], which were obtained with 120 metre moderate-speed cargo ships, without any allowance for air and wave resistances, are also given in this figure.

Wake Tests.

In order to obtain the necessary information for designing propellers, the mean

[3] Rep. Teishinsho Ship Exp. Tank, No. 2 (March 1932), p. 20.

NII-Electronic Library Service

The Society of Naval Architects of Japan

annular wake distribution at the propeller position was measured by blade-wheels on each ship model fitted with all appendages except rudder at a model speed of 1·8 m./sec., corresponding to 16·37 knots of full-sized ship. In Fig. 15 the results are shown in the form of mean annular wake fraction, expressed in terms of model speed, on a base of the radius of annular ring. It will be observed that, broadly speaking, the wake of the ship of smaller resistance is comparatively small, which is quite similar to the result[3] obtained with 120 metre moderate-speed cargo ships.

Propeller Models Employed.

Four speeds of the propeller revolutions at 7,000 S. H. P. were aimed at for each ship, namely, 120, 150, 180 and 210 per minute. All propellers were of the four-bladed type with acrofoil section, the angle of rake being taken as 11°, the expanded area ratio as 0·392 and the blade thickness ratio as 0·045, paying, for the sake of simplicity, no special consideration to strength, cavitation, etc., for full-sized propellers. The dimensions and particulars of sixteen propellers, which were designed by our normal method, whose simplification for the practical uses at ship yards, etc., is described in Appendix, not allowing for so-called "scale effects" between ship and

Prop. No.	R. P. M. aimed at.	Diameter in cm.	Boss ratio.	Pitch ratio (variable) at 0·7 R.	For Ship Model No.
301	120	23·95	0·237	0·784	312
302	150	21·45	0·265	0·699	312
303	180	19·67	0·289	0·636	312
304	210	18·23	0·312	0·574	312
249	120	24·00	0·237	0·784	237
182	150	21·50	0·264	0·708	237
183	180	19·72	0·288	0·648	237
184	210	18·28	0·311	0·580	237
305	120	24·05	0·236	0·786	313
306	150	21·55	0·264	0·701	313
307	180	19·77	0·287	0·640	313
308	210	18·33	0·310	0·580	313
309	120	24·10	0·236	0·789	314
310	150	21·60	0·263	0·704	314
311	180	19·82	0·287	0·644	314
312	210	18·38	0·309	0·582	314

[3] Rep. Teishinsho Ship Exp. Tank, No. 2 (March 1932), p. 20.

NII-Electronic Library Service

The Society of Naval Architects of Japan

model, are shown in the accompanying table, and their general plans are given in Figs. 16 to 31.

Self-Propulsion Tests.

Under the same conditions as those of the resistance tests, each ship model was tested, self-propelled with each of its four propellers, by our normal method for self-propulsion tests, namely, at what is known as the ship point of self-propulsion, not allowing for foul bottom, wind, wave, etc. It should be borne in mind that, since in these tests, for the sake of convenience, the positions of the centres of all propeller models were taken unaltered on ship models irrespectively of the diameters, as shown in Figs. 2 to 5, the working positions of the smaller propellers were too high. Figs. 32 to 35 give the results of these sixteen self-propulsion tests in our standard non-dimensional form, and in Figs. 36 to 39 the curves of S. H. P., R. P. M. and two sets of propulsive coefficients, i. e. η_a=E. H. P. (with appendages)/S. H. P. and η_n=E. H. P. (naked)/S. H. P., of full-sized ships are shown on bases of speed in knots. As seen in these figures, the propeller revolutions at 7,000 S. H. P. do not exactly coincide with those aimed at, the maximum departure being 2 per cent.; hence, in Fig. 40 the attainable speeds and η_a at 7,000 S. H. P. are plotted on a base of R. P. M., and two fair curves are drawn for each ship model. In order to easily obtain the optimum breadths of ships for 7,000 S. H. P., in Fig. 41 the speeds and η_a taken from Fig. 40 for the definite revolutions from 120 to 210 per minute are given on a base of breadth of ship, with optimum lines.

Since, as mentioned above, the maximum departure of measured revolutions from those aimed at is only 2 per cent., in order to find the optimum breadths at various speeds, in Figs. 42 to 45 the shaft horse-powers and η_a for the definite speeds from 13 to 18 knots, directly read from Figs. 36 to 39, are plotted on bases of breadth of ship, and fair curves are drawn, with minimum shaft horse-power lines. In Fig. 46 the optimum breadths for 13 to 18 knots are given on a base of the propeller revolutions designed for 7,000 S. H. P.

Analysing the test results at 16 knots by Froude's method, thrust deduction fraction t, wake fraction w, hull coefficient η_h, propeller efficiency (open) η_p, propeller efficiency (behind) η'_p and relative rotative coefficient η_r, together with shaft horse-power, revolutions per minute and propulsive coefficients, η_n and η_a, are given in the following table.

NII-Electronic Library Service

The Society of Naval Architects of Japan

Model No.	Prop. No.	S.H.P.	N'	η_o	η_i	t	w	η_h	η_p	η'_p	η_r
312	301	5660	111·5	·735	·75	·215	·35	1·21	·61	62	1·02
312	302	5950	142	·695	·71	·20	·36	1·255	·565	57	1·005
312	303	6250	171	·665	·68	·21	·40	1·315	·50	·515	1·03
312	304	6810	208	·61	·62	·205	·425	1·385	·425	·45	1·055
237	249	5350	112	·74	·75	·215	·32	1·155	·625	·65	1·04
237	182	5690	140	·71	·72	·215	·37	1·24	·565	·58	1·025
237	183	5840	170	·675	·685	·215	·38	1·27	·51	·54	1·06
237	184	6360	205·5	·62	·63	·215	·41	1·335	·435	·47	1·085
313	305	5230	110	·755	·765	·20	·34	1·215	·62	·63	1·02
313	306	5450	138·5	·72	·735	·20	·37	1·275	·57	·58	1·02
313	307	5740	170	·685	·70	·19	·37	1·285	·52	·545	1·05
313	308	5990	200·5	·645	·665	·19	·44	1·45	·43	·46	1·075
314	309	5290	110·5	·745	·76	·19	·325	1·20	·625	·635	1·01
314	310	5590	140·5	·70	·715	·20	·35	1·225	·575	·585	1·015
314	311	5890	168	·665	·68	·20	·39	1·32	·51	·515	1·015
314	312	6290	198	·625	·635	·20	·47	1·51	·415	·42	1·01

Conclusions.

(a) As seen in Fig. 41, the attainable speeds at 7,000 S. H. P. for the same revolutions quickly increase at first and then gradually fall off with the increase of the breadth of ship.

(b) As seen in Fig. 41, when the breadth of ship is between 17·5 m. and 18·5 m., the propulsive coefficients at 7,000 S. H. P. are roughly constant for the same revolutions, while, when the breadth becomes greater, they increase at first and then fall off with the increase of breadth.

(c) As seen in Fig. 41, the optimum breadth at 7,000 S. H. P. gradually decreases at first and then becomes approximately constant with the increase of propeller revolutions.

(d) Though, when the air resistance is taken into consideration, the optimum breadth should become smaller than given in Fig. 41, as it could be clearly supposed from Fig. 14, which shows the breadth of minimum resistance for various wind velocities, it may be generally said that the optimum breadth is somewhat greater than in current practice, provided that the displacement and draught be kept unaltered.

(e) As seen in Figs. 42 to 45, the optimum breadth for each revolutions designed

NII-Electronic Library Service

The Society of Naval Architects of Japan

for 7,000 S. H. P. slightly decreases at first and then becomes approximately constant with the decrease of speed.

(f) As seen in Fig. 46, the optimum breadths at any speeds decrease at first and then become approximately constant with the increase of propeller revolutions.

(g) Broadly speaking, since the breadths of minimum resistance and maximum propulsive coefficient could be said to be roughly identical, as seen in Figs. 14 and 42 to 45, the breadth of minimum resistance may be generally considered as the optimum breadth for propulsive economy.

(h) As seen in Figs. 36 to 39, the adoption of large slow-running propellers always improves the propulsive performance considerably.

(i) The table, giving the analysed results by Froude's method, shows that all the coefficients, fractions and efficiencies do not materially change their values with the breadth of ship.

It should be remembered that these conclusions cannot be absolutely true, unless all the propellers employed were the optimum under the given conditions. Experience has shown that the propellers designed by our method may be generally said to be quite close to the optimum, though, strictly speaking, they may not be the optimum. Therefore, I believe that the above conclusions can apply approximately to all ships similar to those dealt with in the present research.

Lastly, I wish to acknowledge my indebtedness to Messrs. H. Shiba, T. Kitashima and E. Morisaki for their assistances in preparing this paper.

APPENDIX.

Approximate Method of Obtaining Induced Pitch Angles.

In order to design the optimum wake propellers under the given conditions, we always determine at first the induced or hydrodynamic pitch angles β_{ri} by Dr. Shigemitsu's method[4]. Since it is laborious to find the values of β_{ri} by this metod, I intended to present the diagrams to be utilized for the easy determination of their approximate values, which, however, are accurate enough to be used for propeller designers, such as at ship yards, who have no means of obtaining the accurate wake distributions at propeller positions. If the number of propeller blades, the boss ratio and the radial distribution of mean annular wakes, together with drag-lift ratios of blade sections to be used, are given, the induced advance ratio $\tan\beta_{ri}$ is a function

[4] Rep. Teishinsho Ship Exp. Tank, No. 1 (Sept. 1931), p. 1.

NII-Electronic Library Service

The Society of Naval Architects of Japan

of the advance ratio $\tan\beta_r=\frac{V_{ra}}{r\omega}$ and the thrust constant $t=\frac{T}{\rho N^2D^4}$ only. Examining the wake distributions measured with about one hundred ship models, the average wake distributions of single- and twin-screw ships were determined as shown by full and broken lines, respectively, in Fig. 47. Since the wake distributions of single-screw ships were found to vary widely with the shape of their frame-lines, etc., two limiting curves for their wake distributions were also shown by dotted and broken lines in Fig. 47, the latter coinciding with an average line for twin-screw ships. For 4-bladed propellers with the boss ratio of 0·22 to work in three different wake distributions given in Fig. 47, the values of $\tan\beta_{ri}$ for $t=0{\cdot}10$, 0·15, 0·20, 0·25, 0·30 and 0·35, which cover fully the practical range of thrust constant, were calculated for the various values of $\tan\beta_r$. In this calculation, according to our current practice, the drag-lift ratio of blade sections were taken as 0·055. In Fig. 48 the results are given on bases of $\tan\beta_r$. Since the values of $\tan\beta_{ri}$ are hardly affected by boss ratio, the diagrams given in Fig. 48 are approximately applicable to all 4-bladed propellers of single- and twin-screw ships, provided that, for single-screw ships with extraordinary shape of frame-lines, the suitable wake distributions be assumed and the interpolation of $\tan\beta_{ri}$ be made between three sets of the curves of $\tan\beta_{ri}$.

I wish to express my best thanks to Mr. T. Kiyota for his labour in numerical calculations.

NII-Electronic Library Service

The Society of Naval Architects of Japan

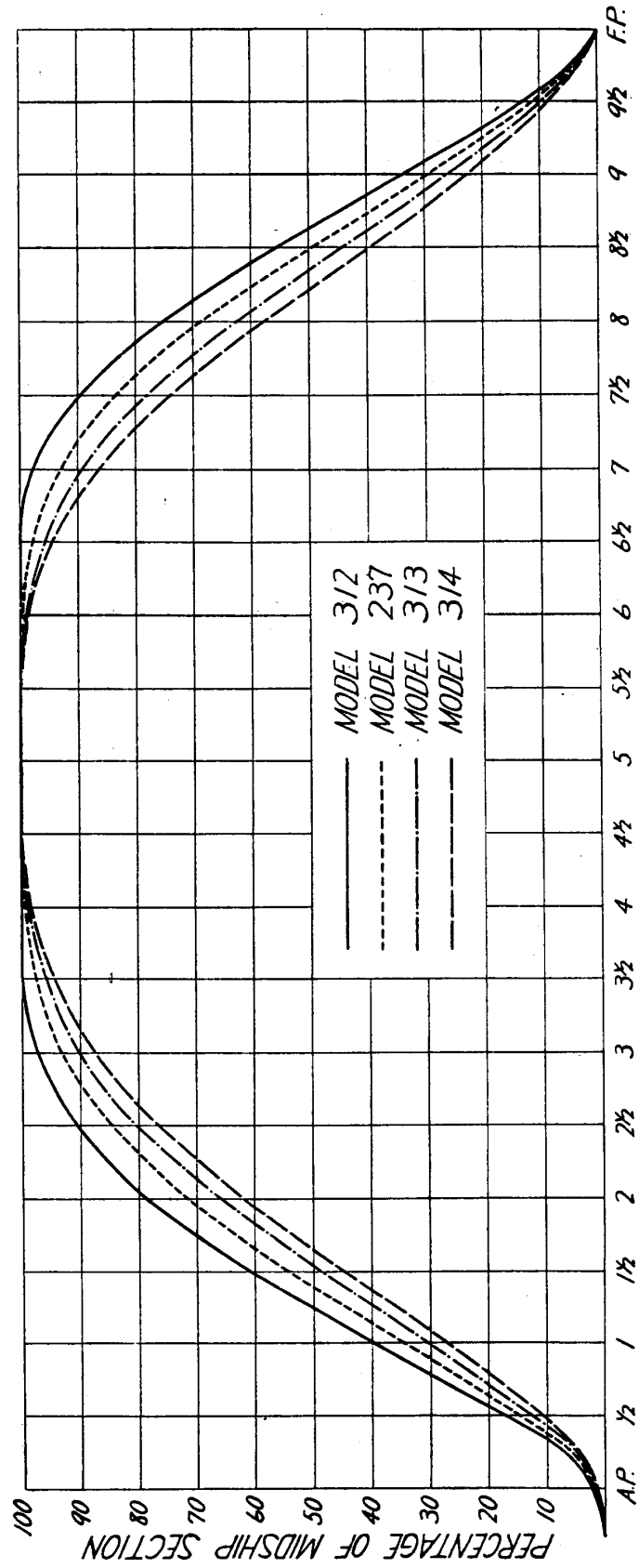

FIG. 1.— SECTIONAL AREA CURVES.

NII-Electronic Library Service

The Society of Naval Architects of Japan

BODY PLAN

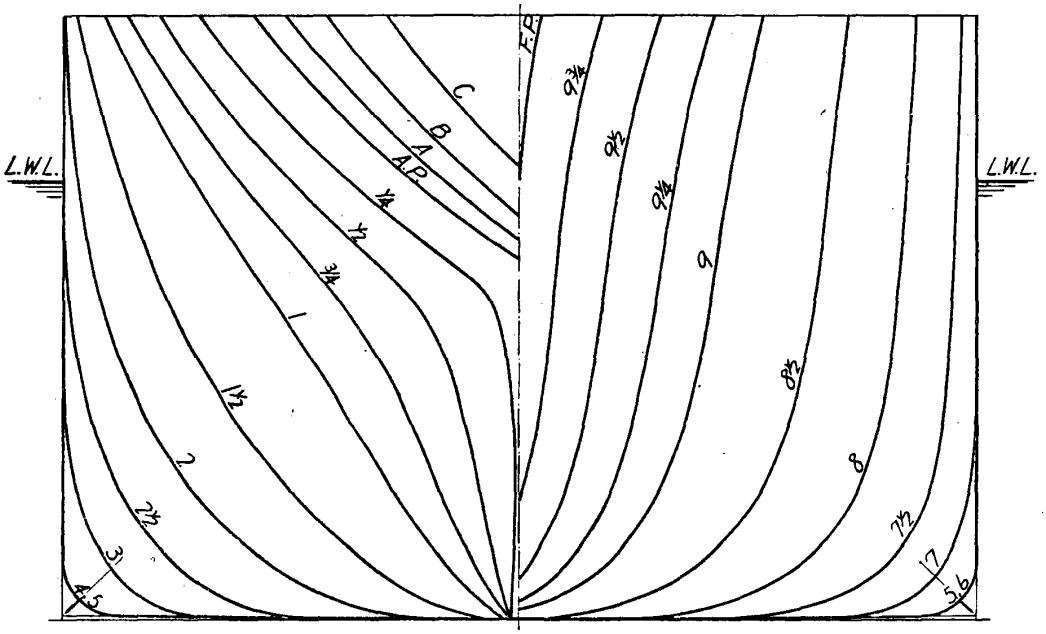

BOW AND STERN ARRANGEMENTS

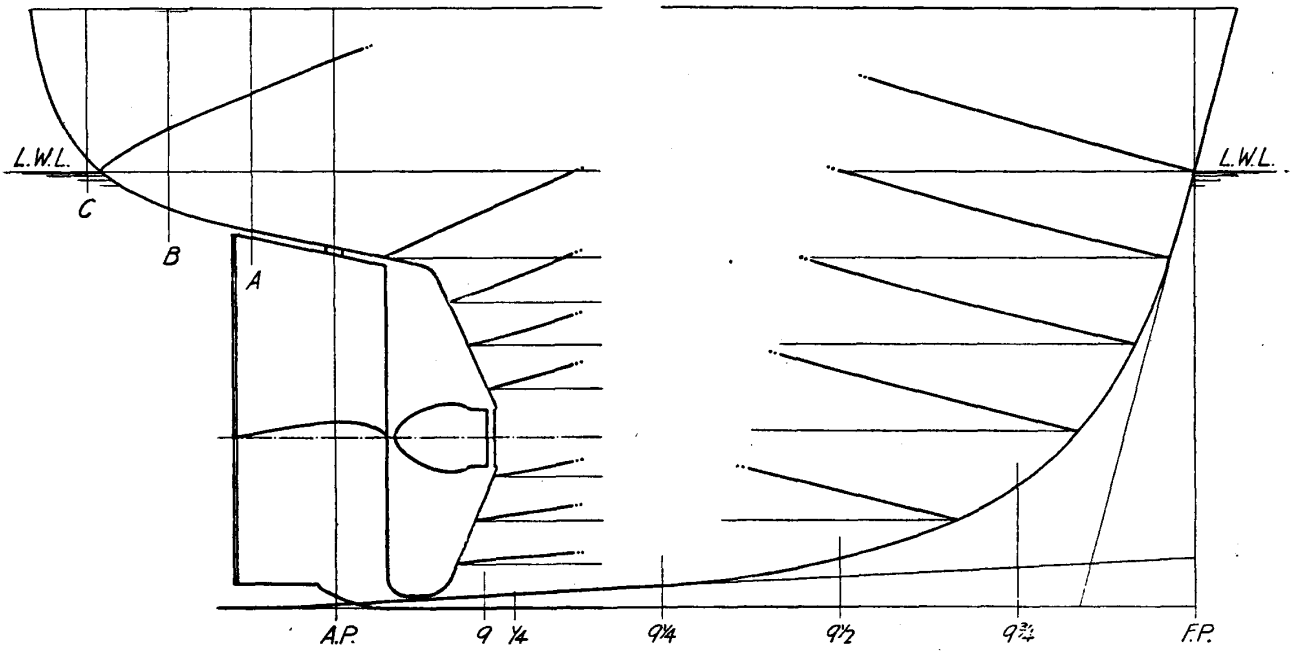

FIG. 2.—SHIP MODEL 312.

NII-Electronic Library Service

The Society of Naval Architects of Japan

BODY PLAN

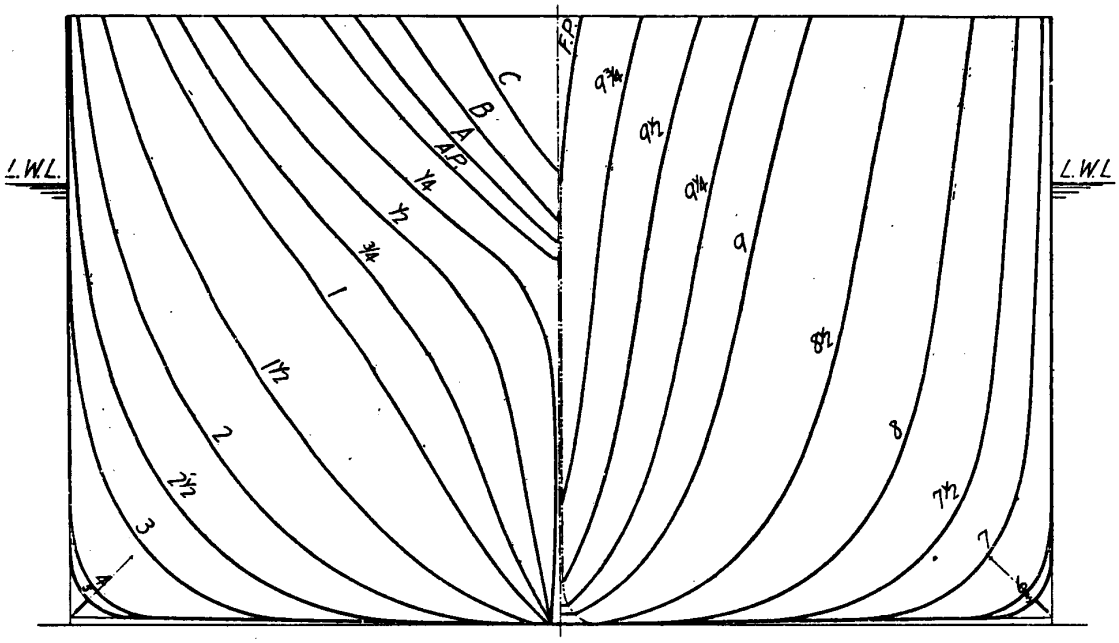

BOW AND STERN ARRANGEMENTS

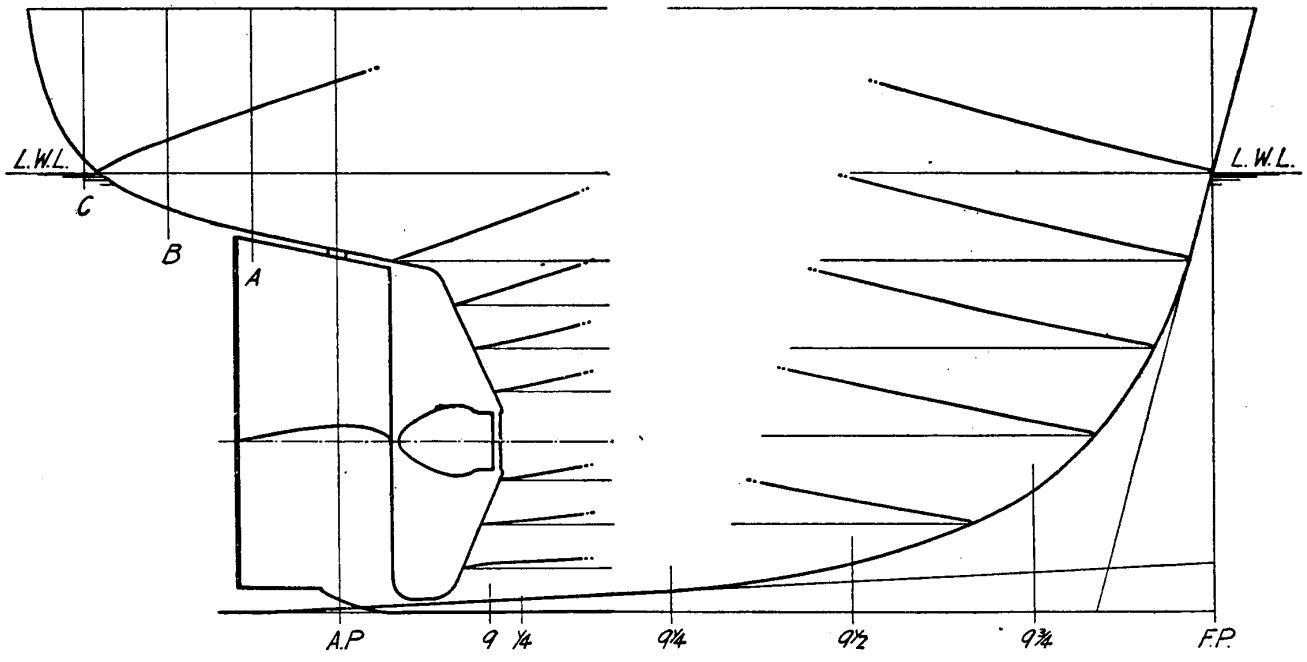

FIG. 3.— SHIP MODEL 237

NII-Electronic Library Service

The Society of Naval Architects of Japan

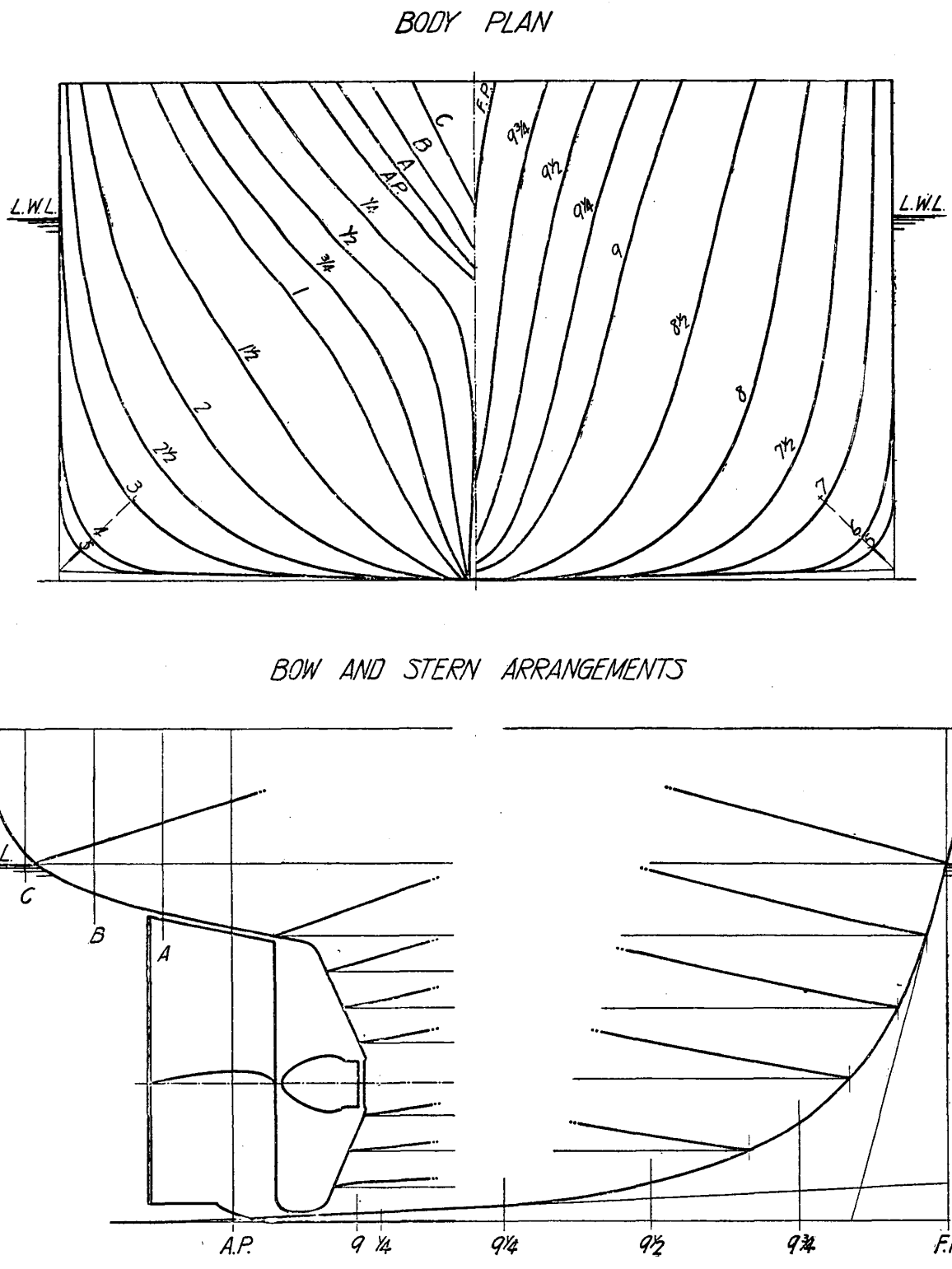

FIG. 4.—SHIP MODEL 313.

NII-Electronic Library Service

The Society of Naval Architects of Japan

BODY PLAN

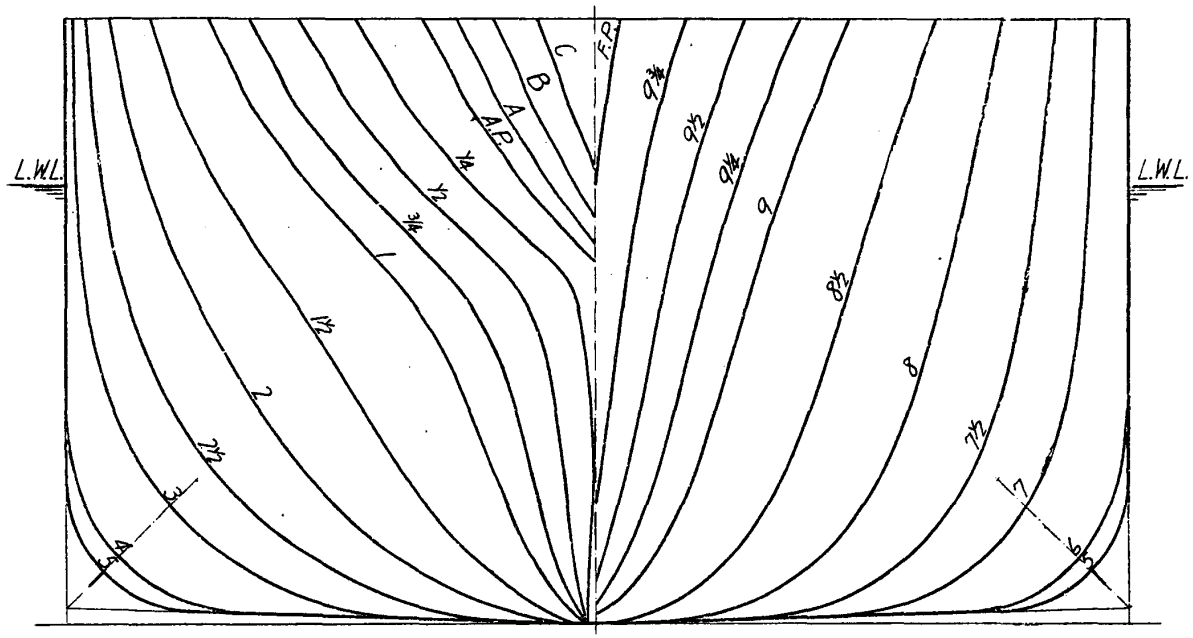

BOW AND STERN ARRANGEMENTS

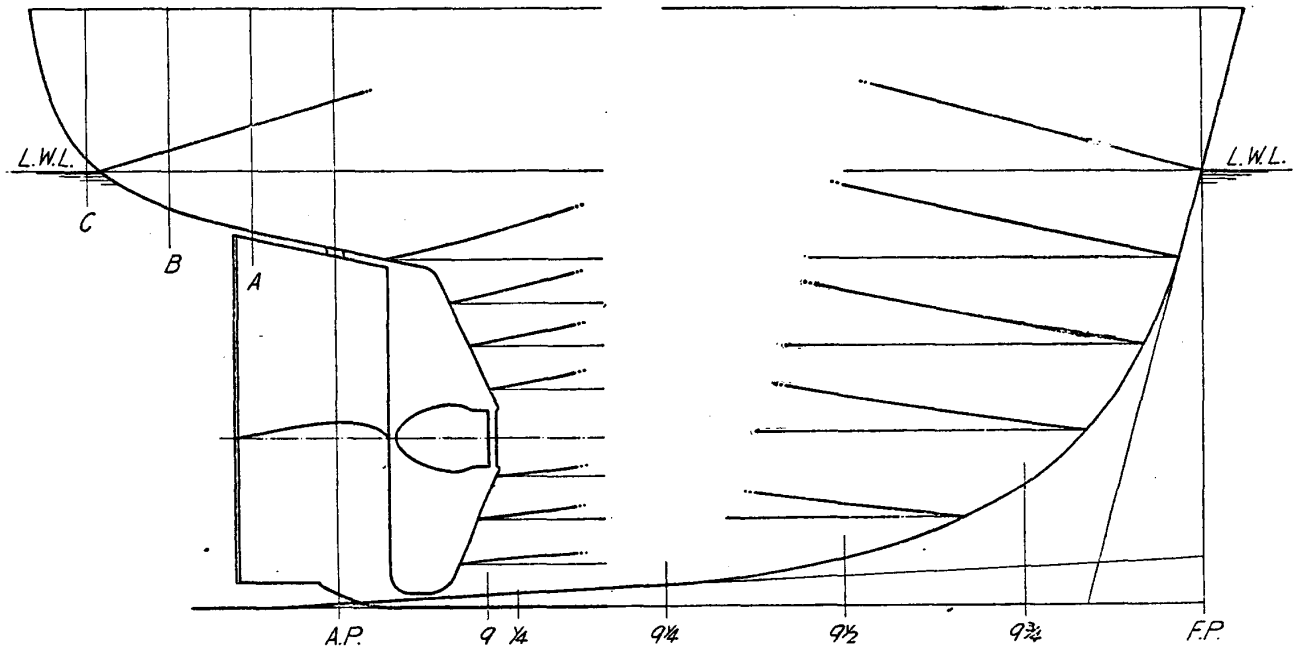

FIG. 5. — SHIP MODEL 314.

NII-Electronic Library Service

The Society of Naval Architects of Japan

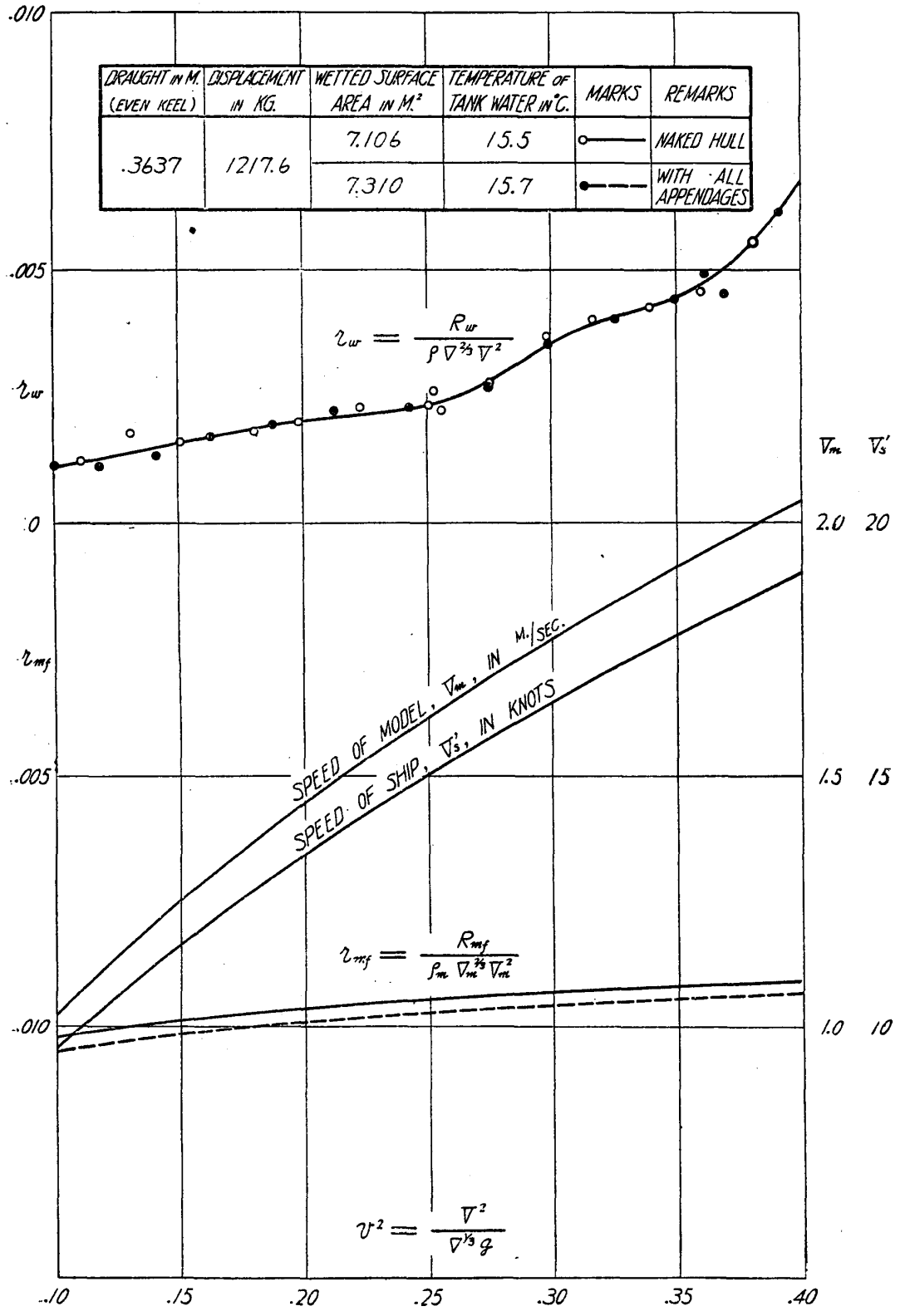

FIG. 6.— RESULTS OF RESISTANCE TESTS OF MODEL 312.

NII-Electronic Library Service

The Society of Naval Architects of Japan

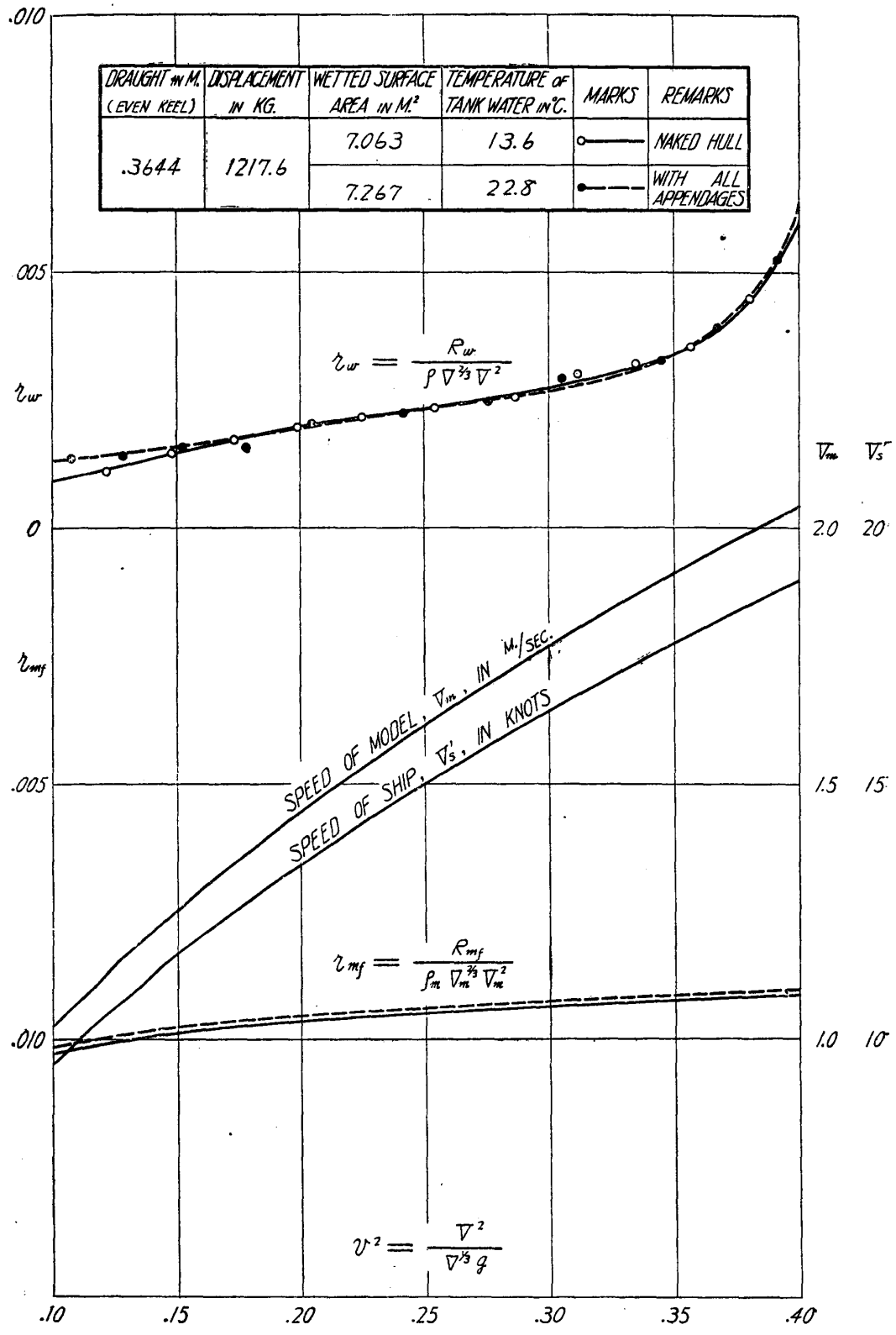

FIG. 7.— RESULTS OF RESISTANCE TESTS OF MODEL 237.

NII-Electronic Library Service

The Society of Naval Architects of Japan

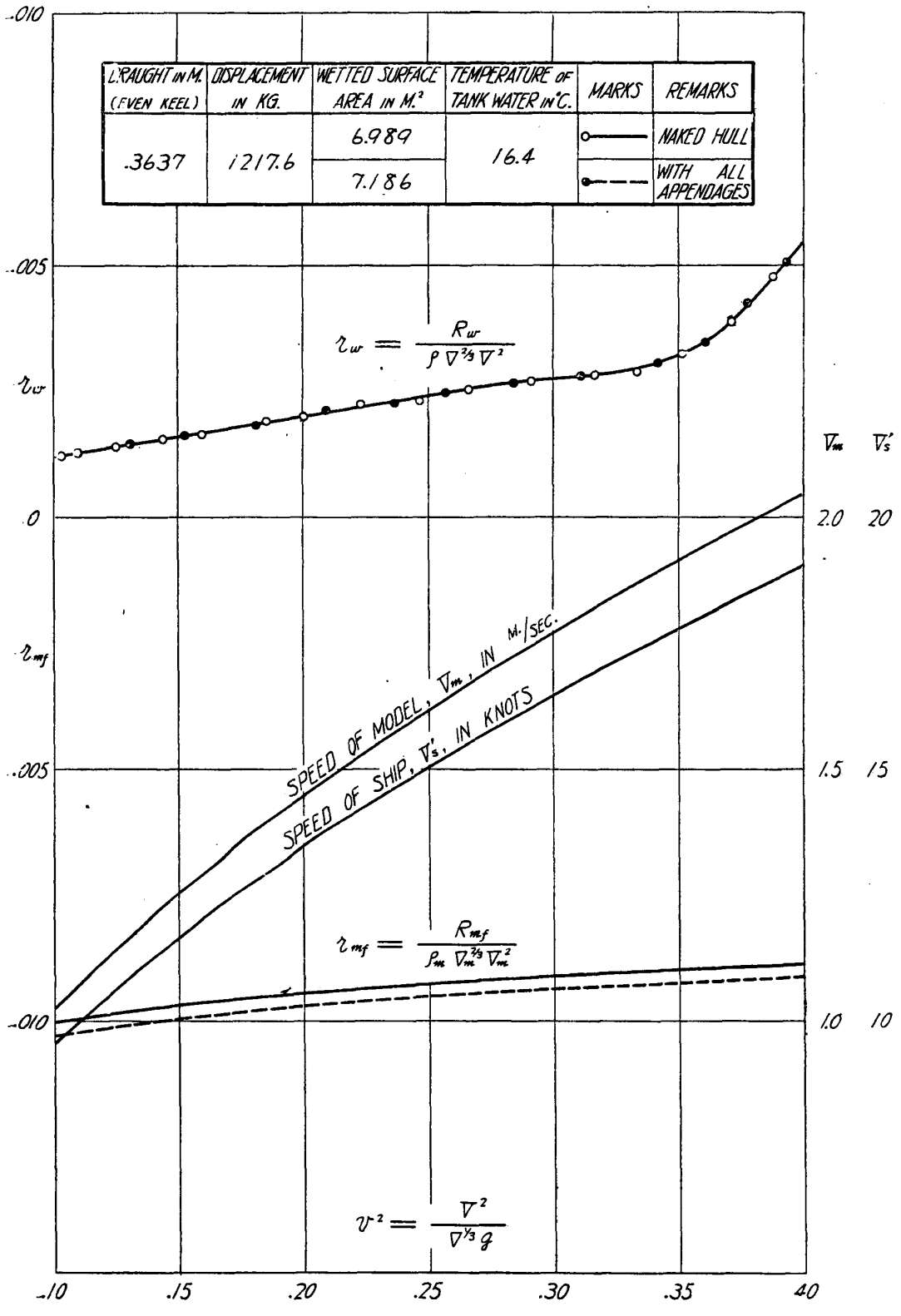

FIG. 8.— RESULTS OF RESISTANCE TESTS OF MODEL 313.

NII-Electronic Library Service

The Society of Naval Architects of Japan

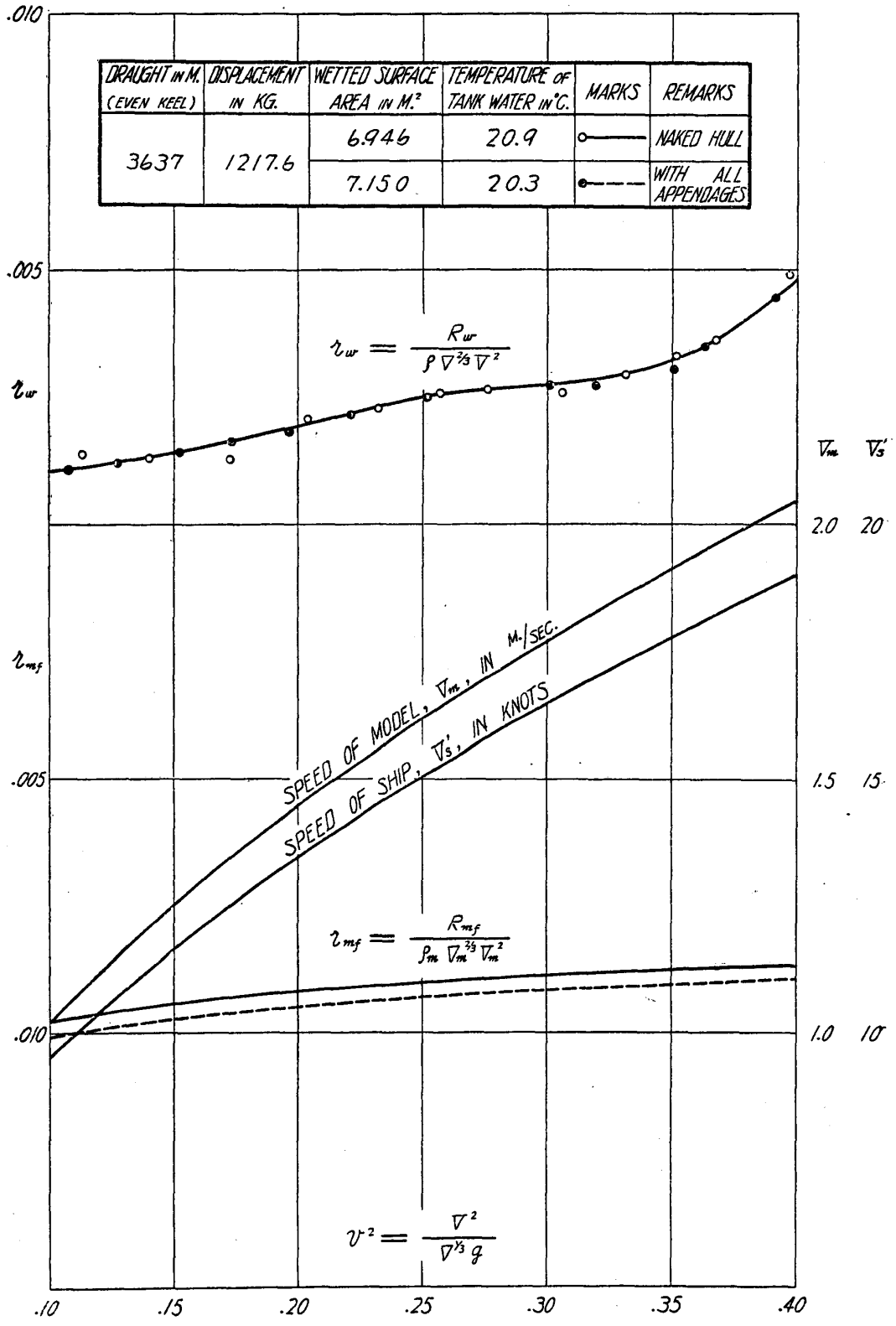

FIG. 9.— RESULTS OF RESISTANCE TESTS OF MODEL 314.

NII-Electronic Library Service

The Society of Naval Architects of Japan

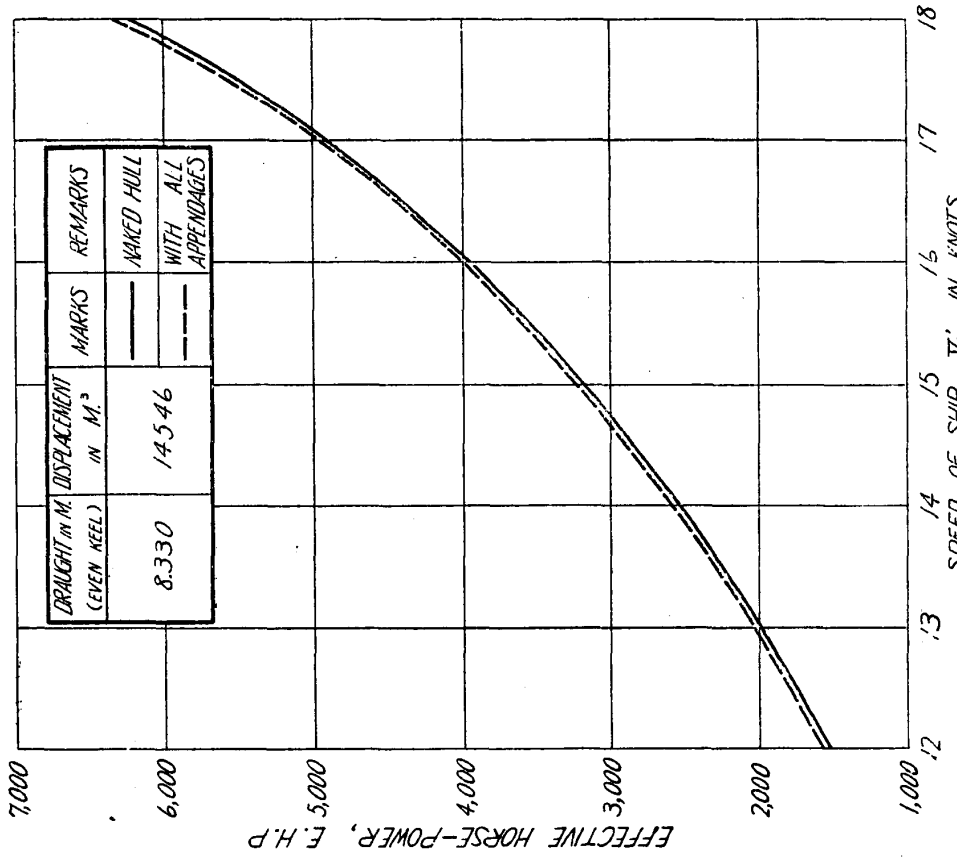

FIG. 11. — E.H.P. CURVES OF MODEL 237.

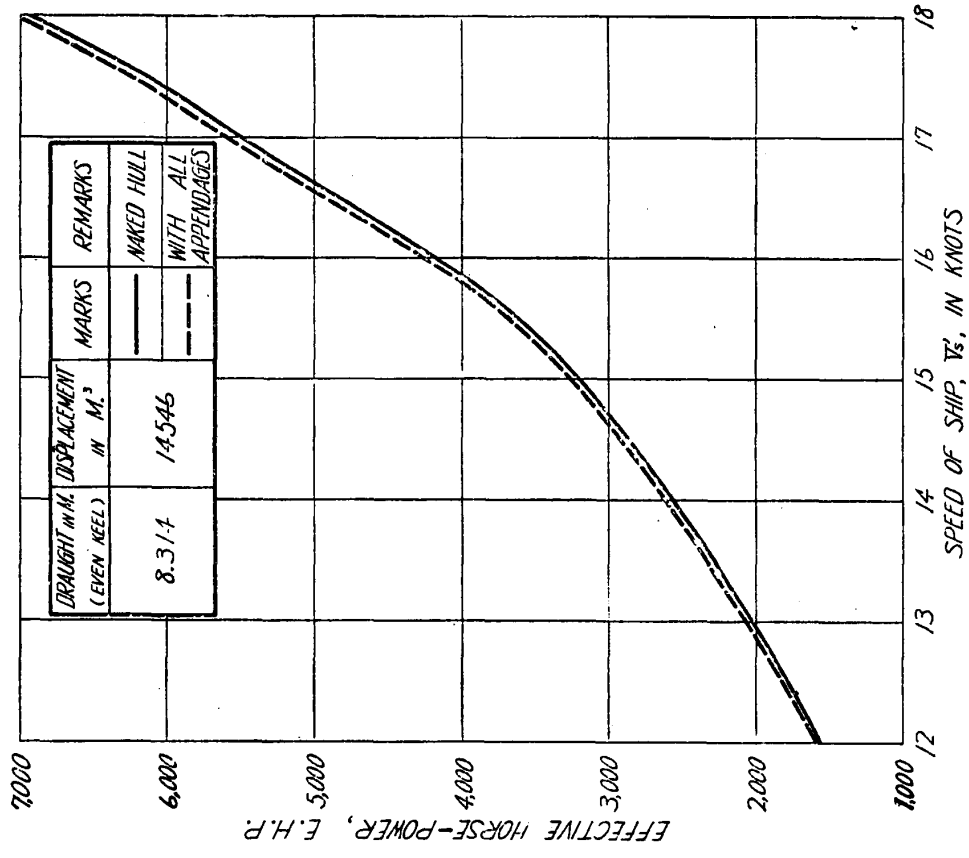

FIG. 10. — E.H.P. CURVES OF MODEL 312.

NII-Electronic Library Service

The Society of Naval Architects of Japan

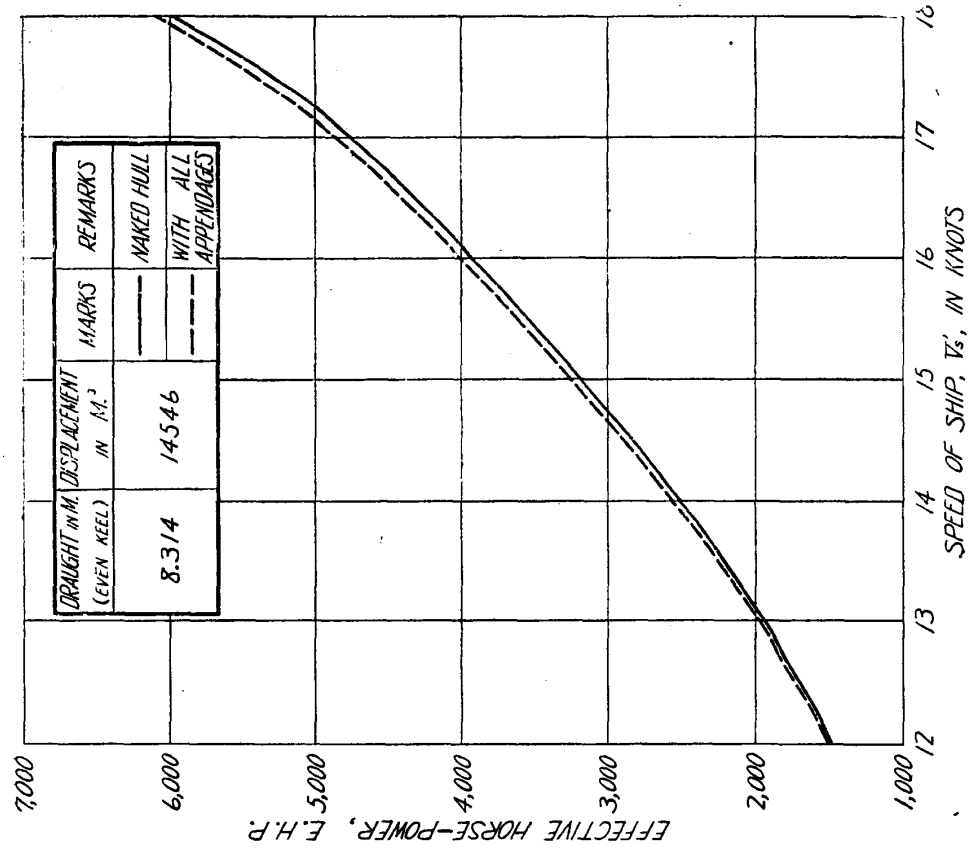

FIG. 13.— E.H.P. CURVES OF MODEL 3/4.

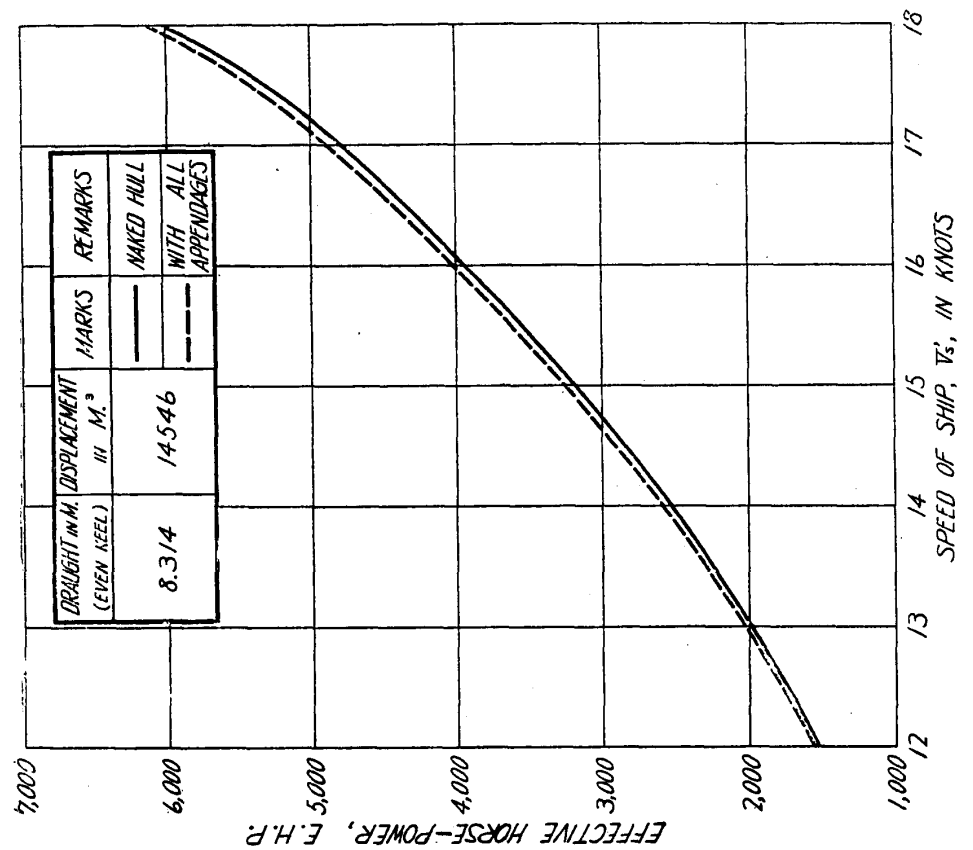

FIG. 12.— E.H.P. CURVES OF MODEL 3/3.

NII-Electronic Library Service

The Society of Naval Architects of Japan

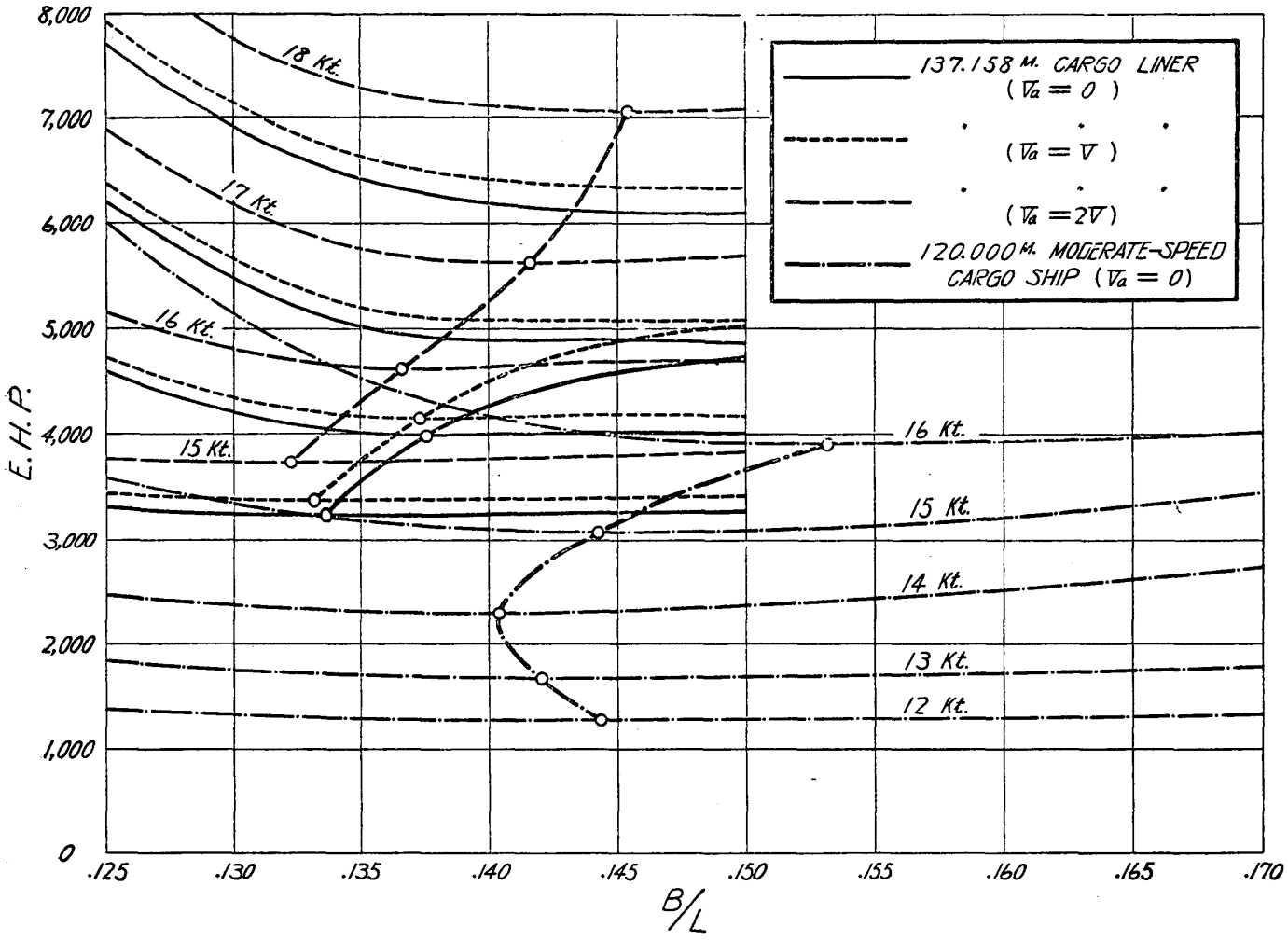

FIG. 14.— BREADTH OF MINIMUM RESISTANCE.

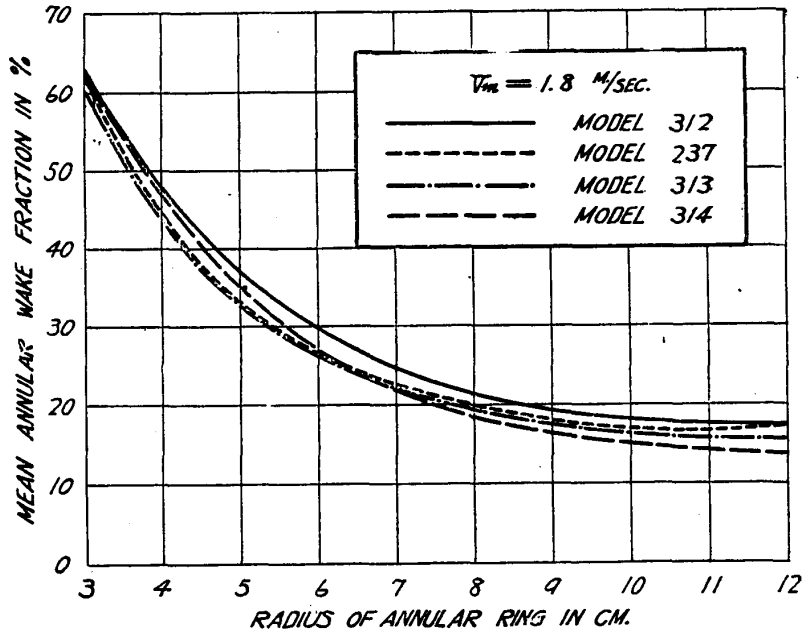

FIG. 15.— MEAN ANNULAR WAKE DISTRIBUTIONS.

NII-Electronic Library Service

The Society of Naval Architects of Japan

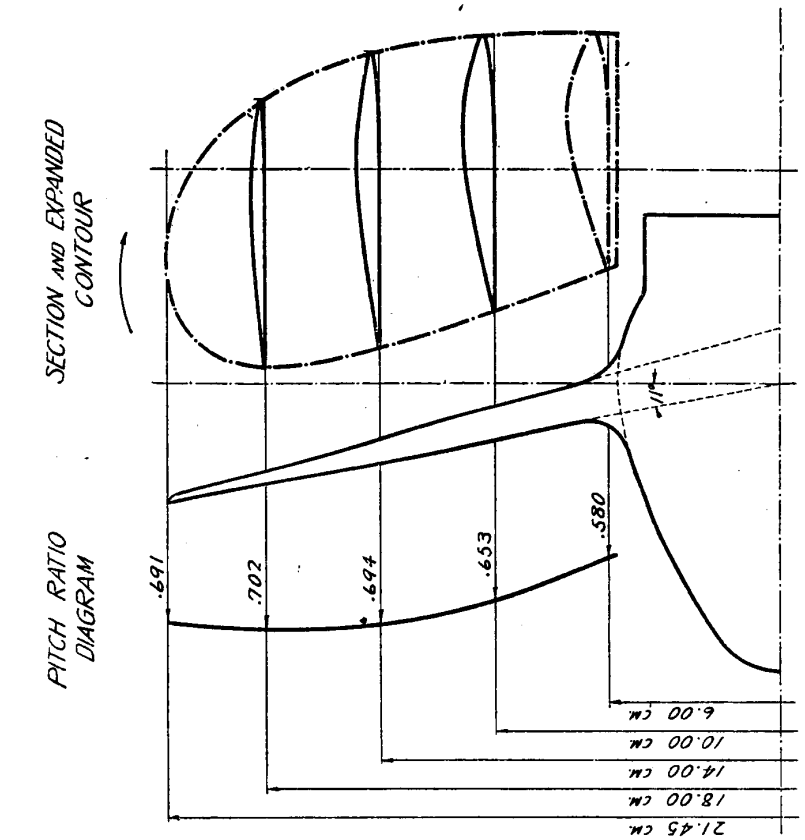

FIG. 17.— PROPELLER 302.

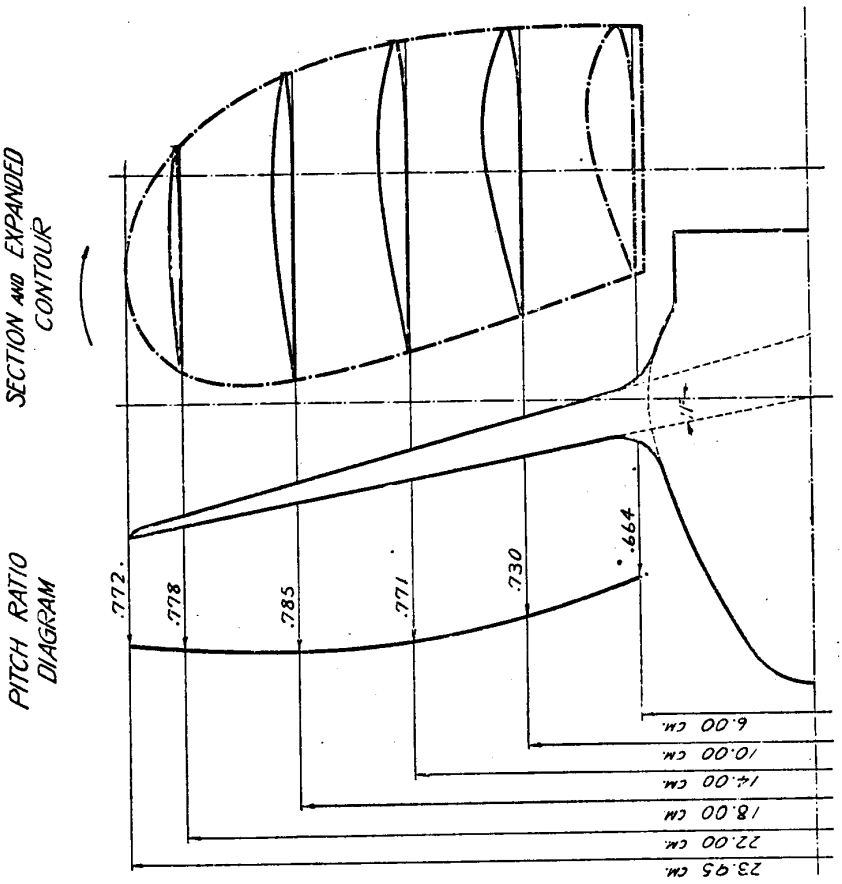

FIG. 16.— PROPELLER 301.

NII-Electronic Library Service

The Society of Naval Architects of Japan

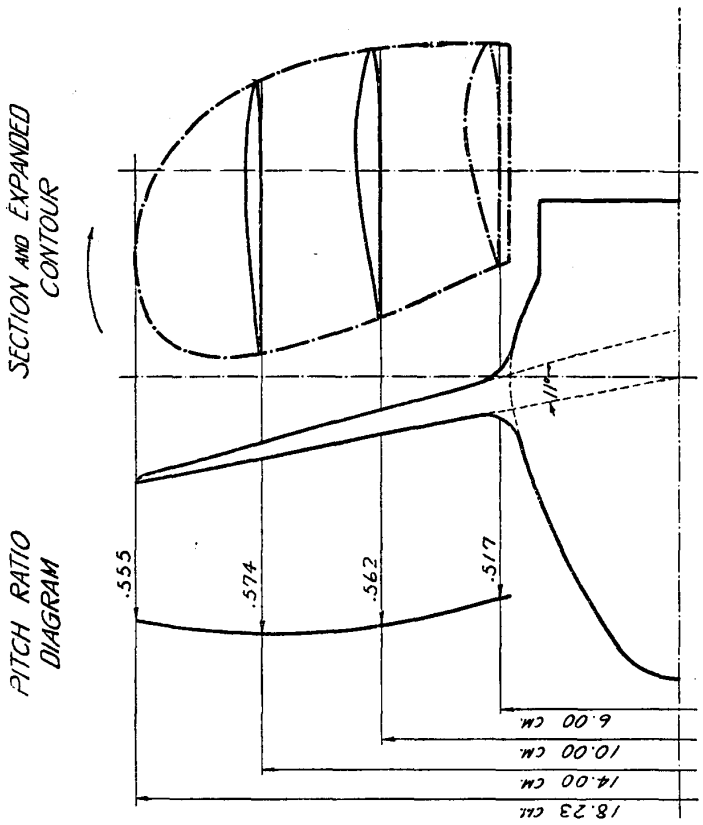

FIG. 19.— PROPELLER 304.

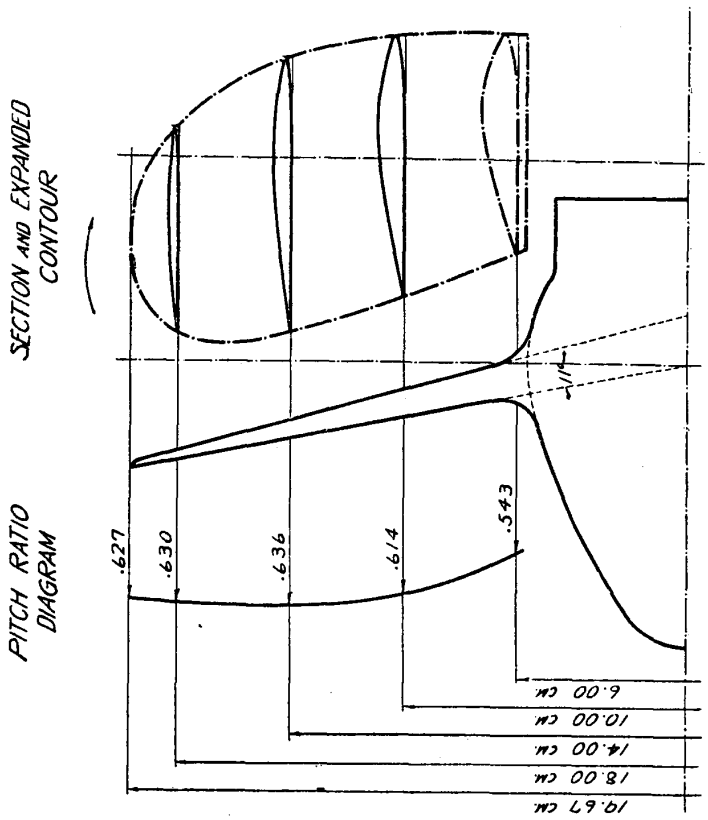

FIG. 18.— PROPELLER 303.

NII-Electronic Library Service

The Society of Naval Architects of Japan

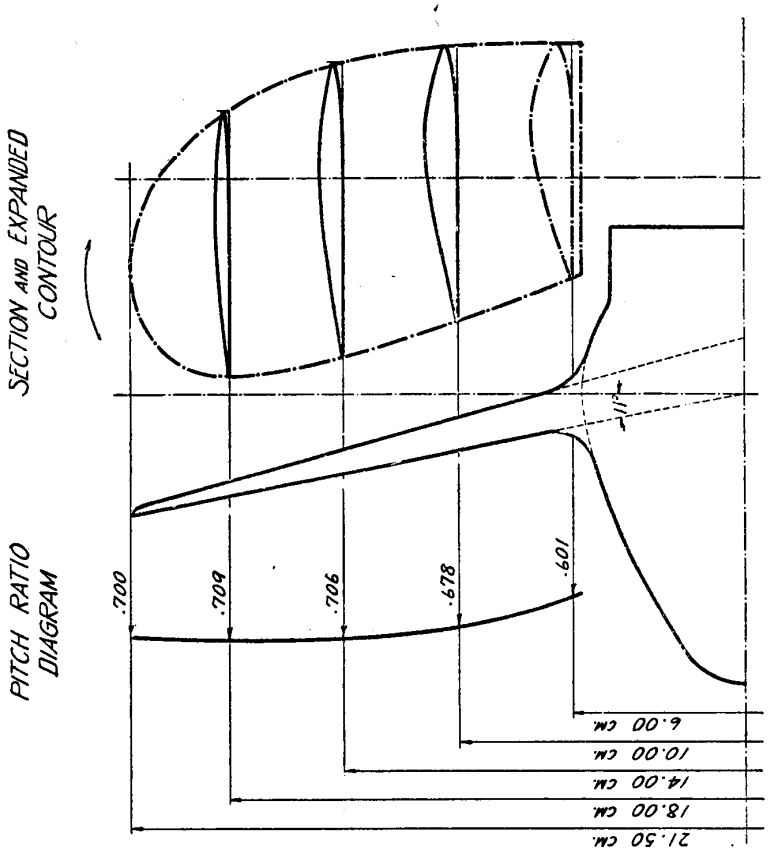

FIG. 21.— PROPELLER 182.

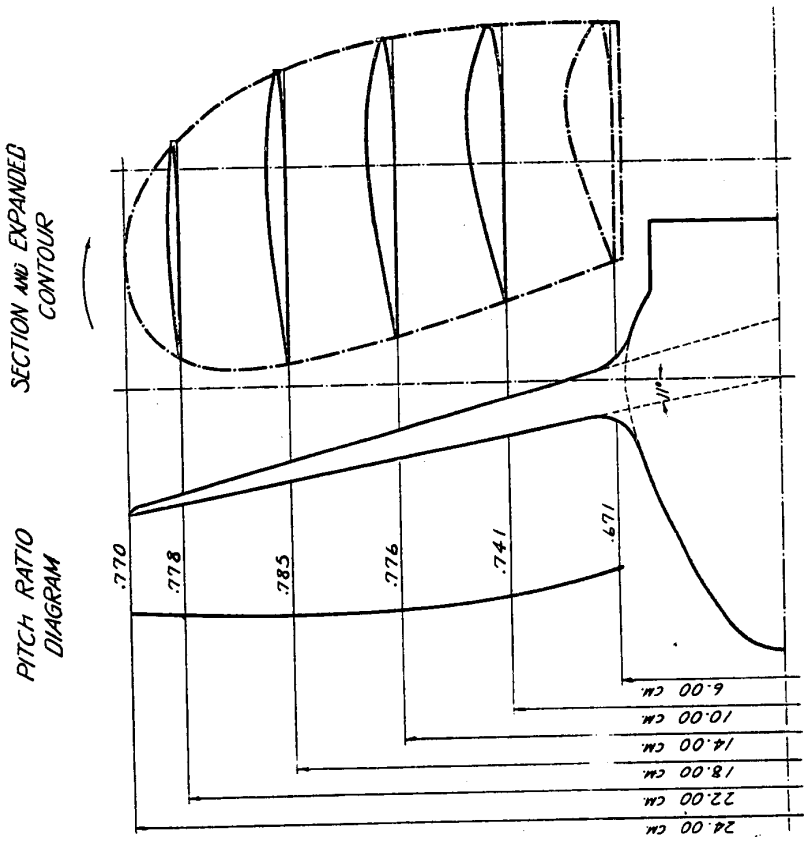

FIG. 20.— PROPELLER 249.

NII-Electronic Library Service

The Society of Naval Architects of Japan

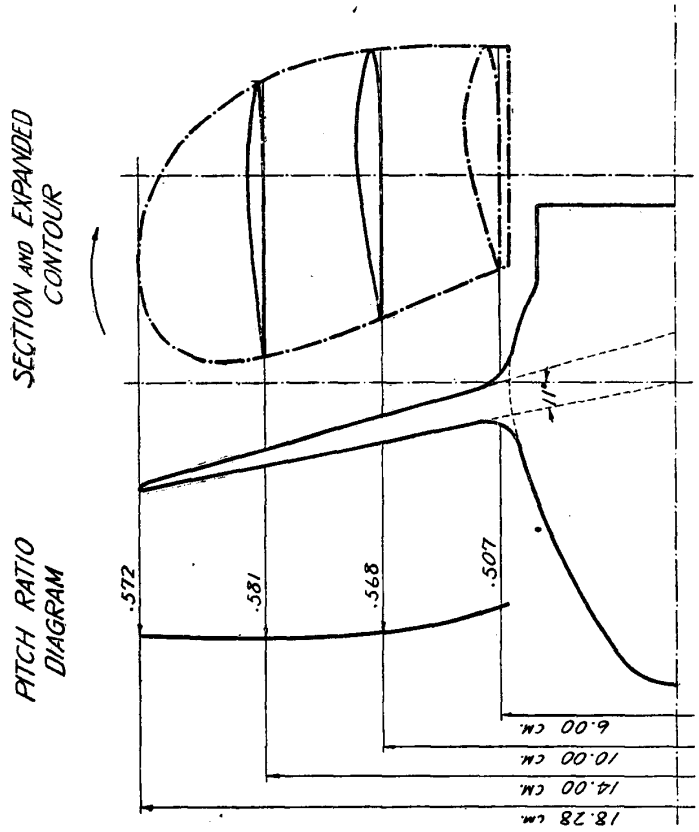

FIG. 23.— PROPELLER 184.

FIG. 25.— PROPELLER 306.

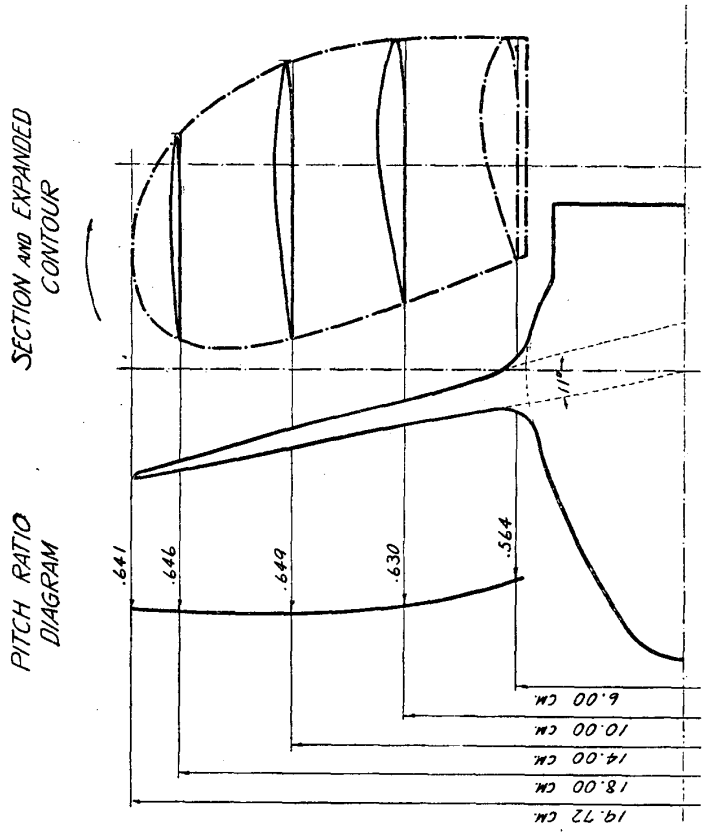

FIG. 22.— PROPELLER 183.

NII-Electronic Library Service

The Society of Naval Architects of Japan

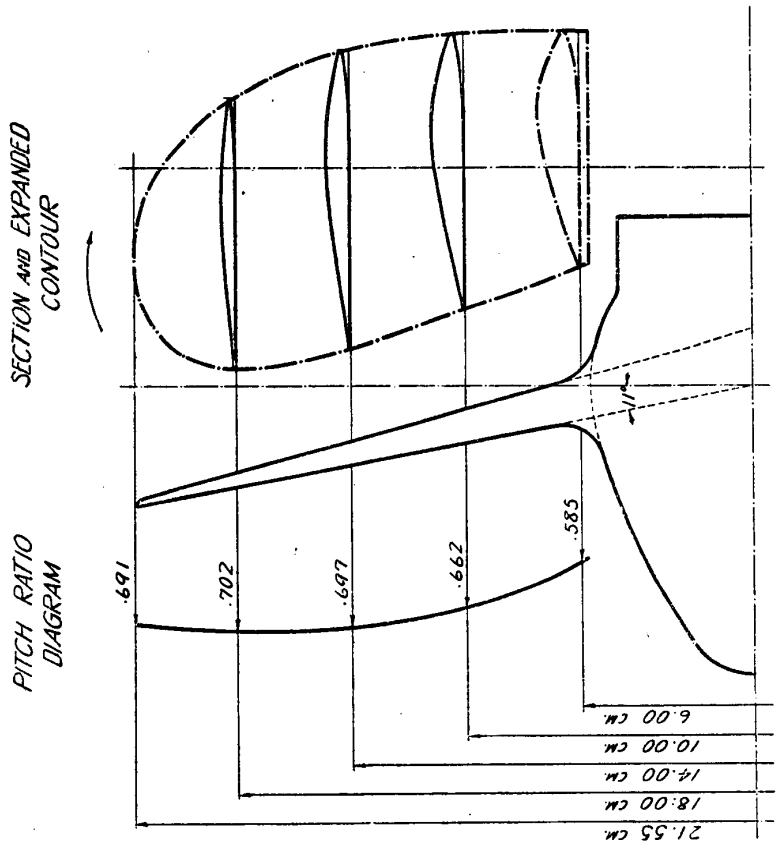

FIG. 25.— PROPELLER 306.

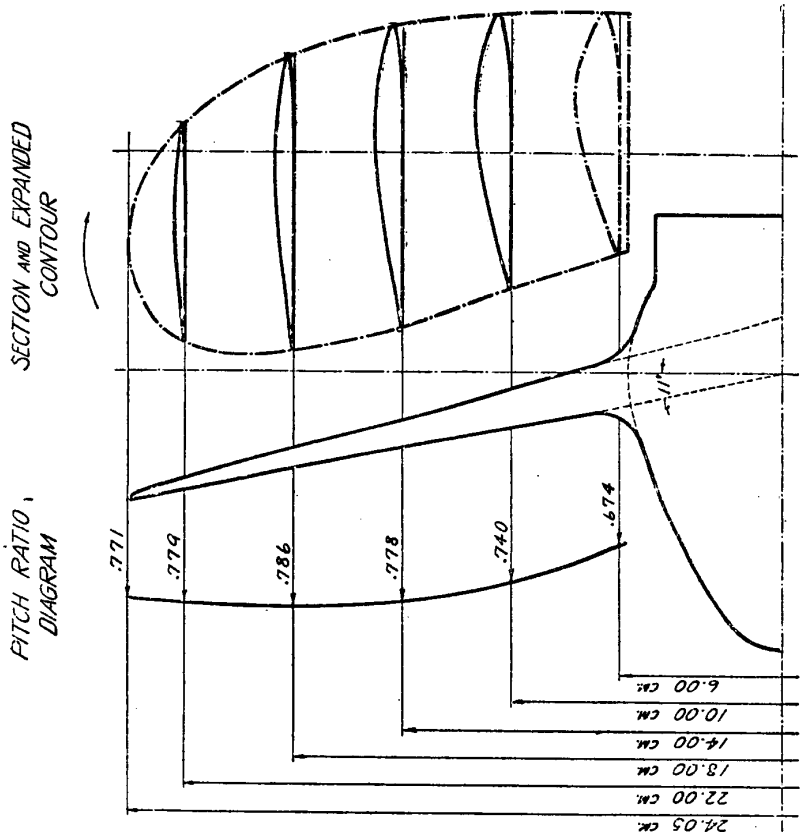

FIG. 24.— PROPELLER 305.

NII-Electronic Library Service

The Society of Naval Architects of Japan

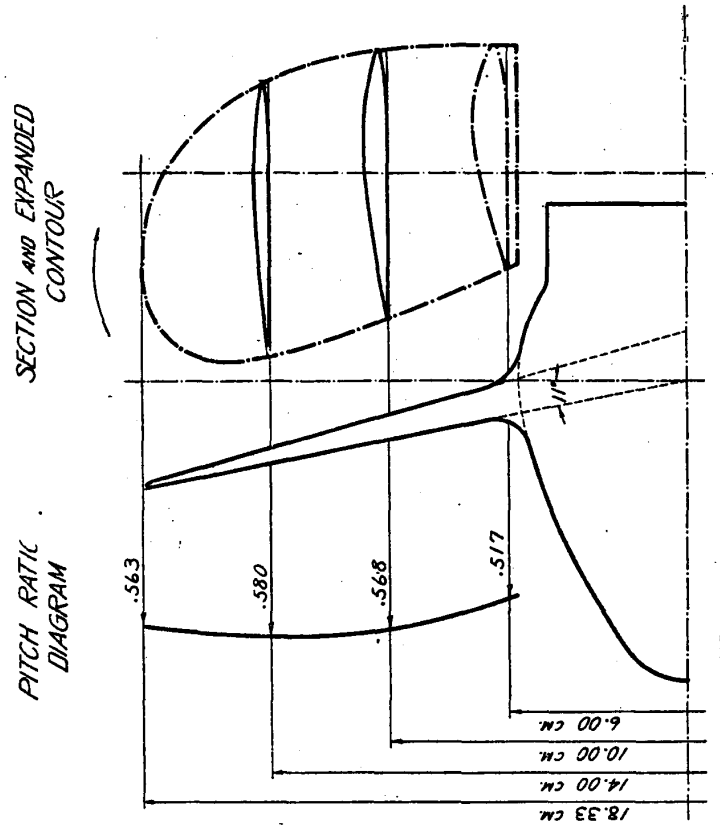

FIG. 27.— PROPELLER 308.

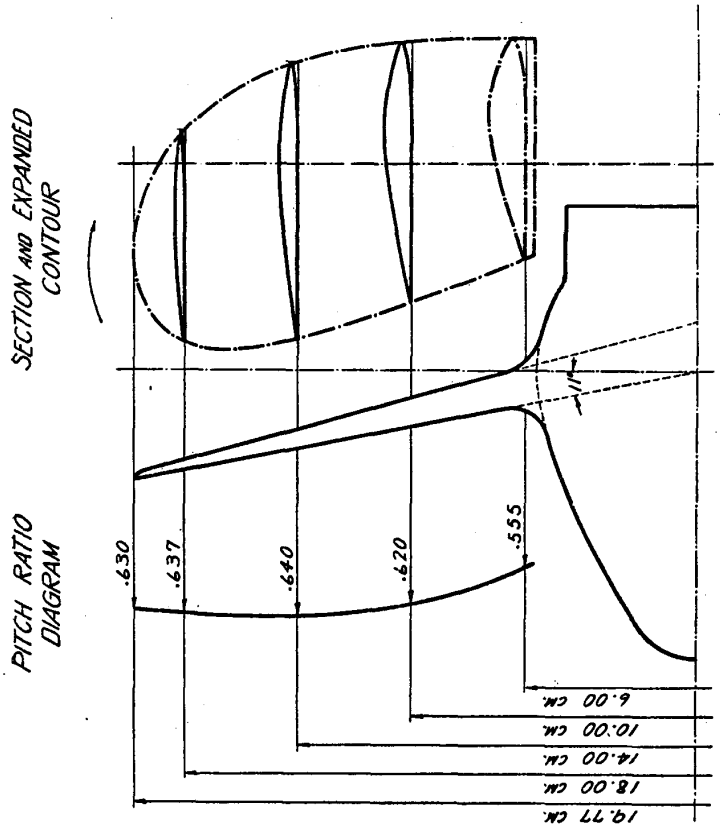

FIG. 26.— PROPELLER 307.

NII-Electronic Library Service

The Society of Naval Architects of Japan

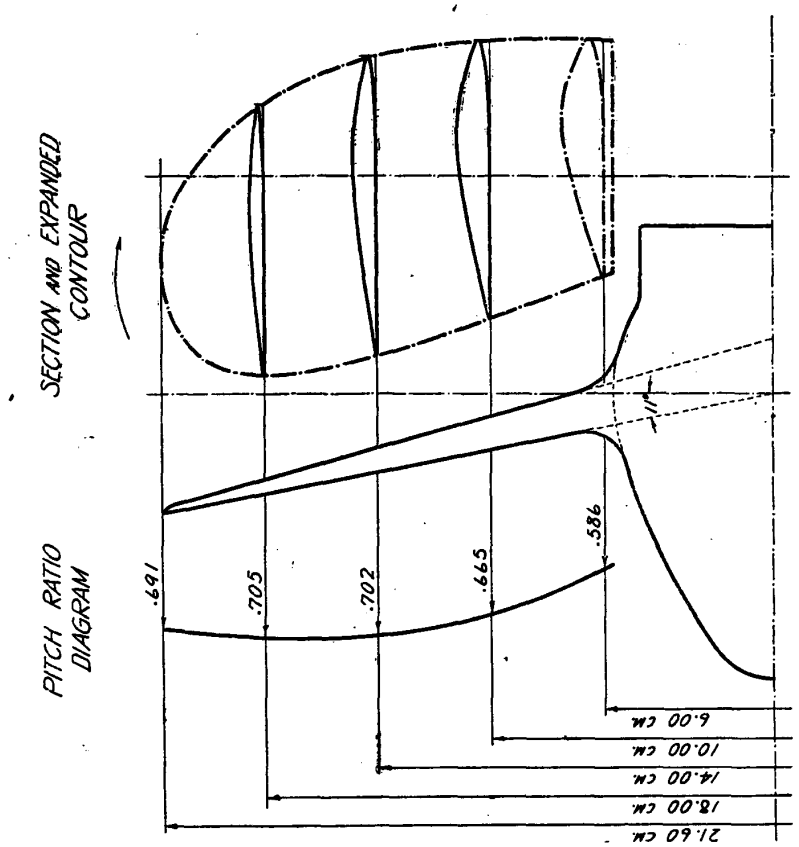

FIG. 29.— PROPELLER 310.

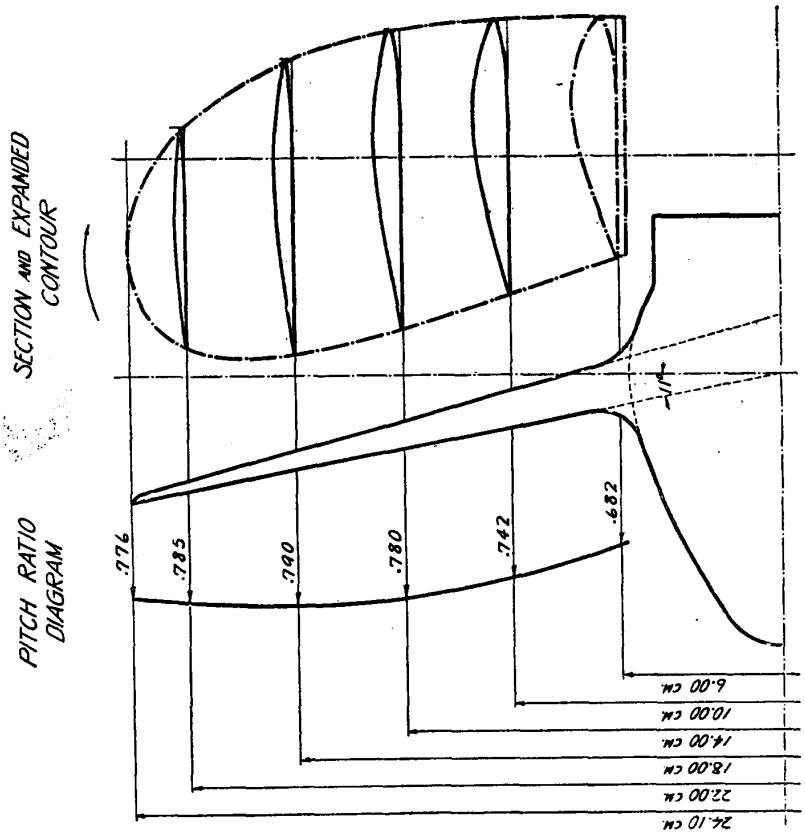

FIG. 28.— PROPELLER 309.

NII-Electronic Library Service

The Society of Naval Architects of Japan

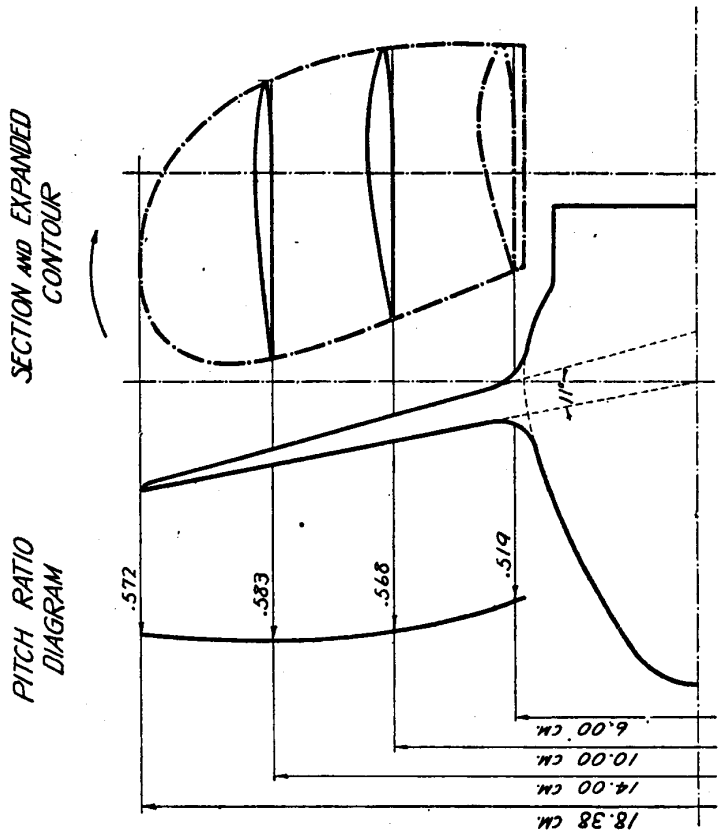

FIG. 31.— PROPELLER 312.

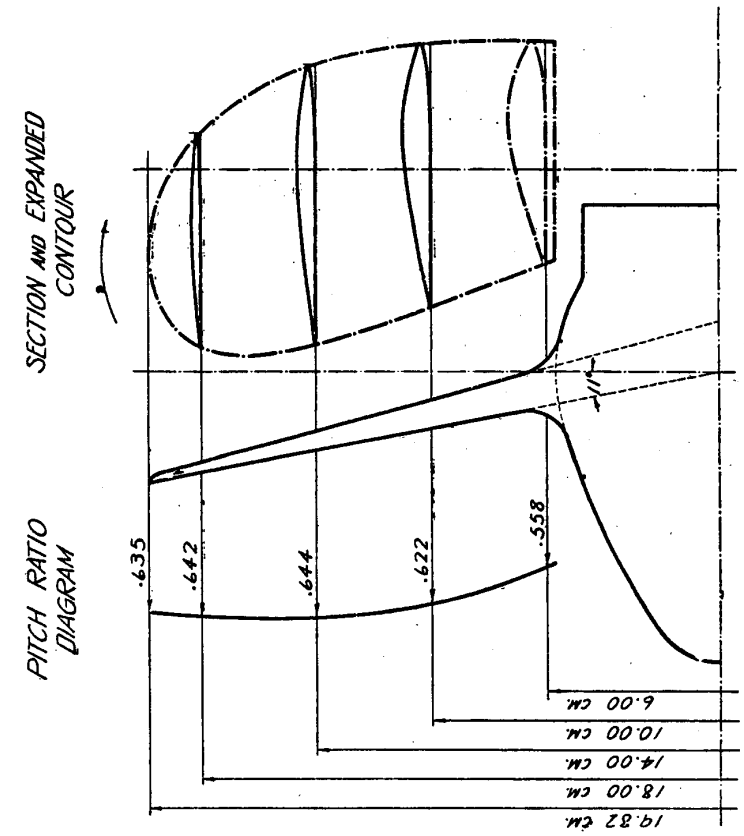

FIG. 30.— PROPELLER 311.

NII-Electronic Library Service

The Society of Naval Architects of Japan

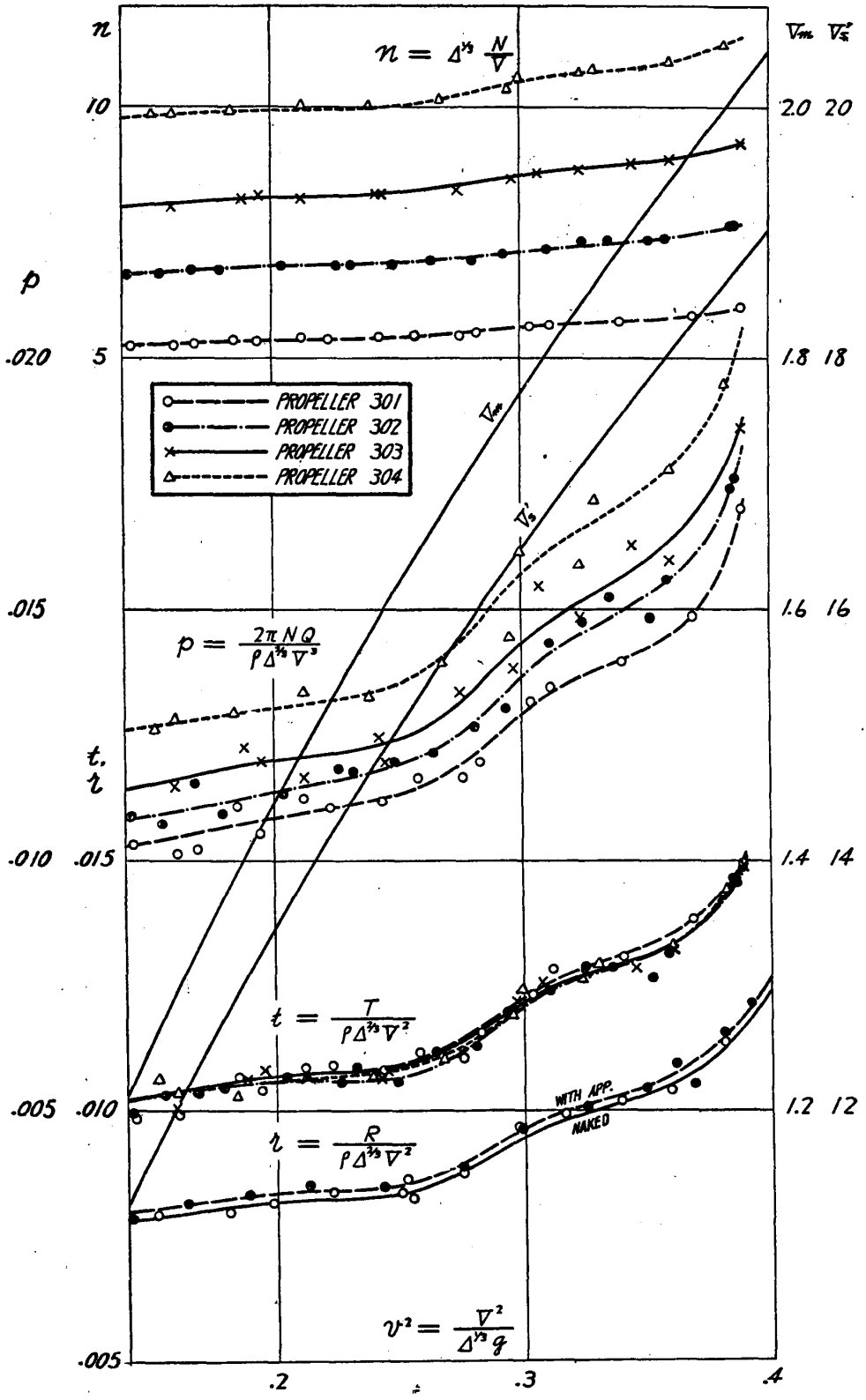

FIG. 32.—RESULTS OF SELF-PROPULSION TESTS OF MODEL 312.

NII-Electronic Library Service

The Society of Naval Architects of Japan

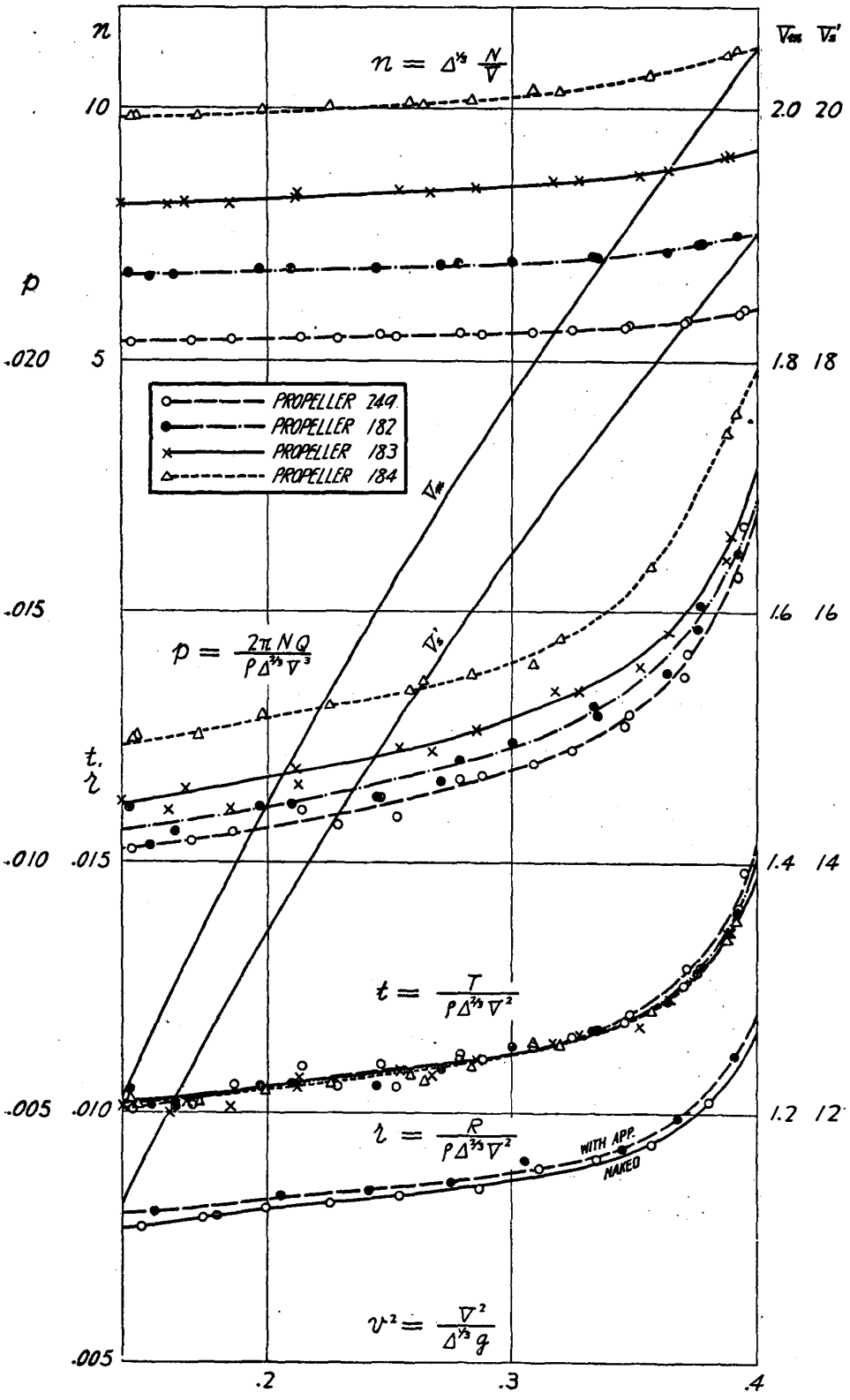

FIG. 33.—RESULTS OF SELF-PROPULSION TESTS OF MODEL 237.

NII-Electronic Library Service

The Society of Naval Architects of Japan

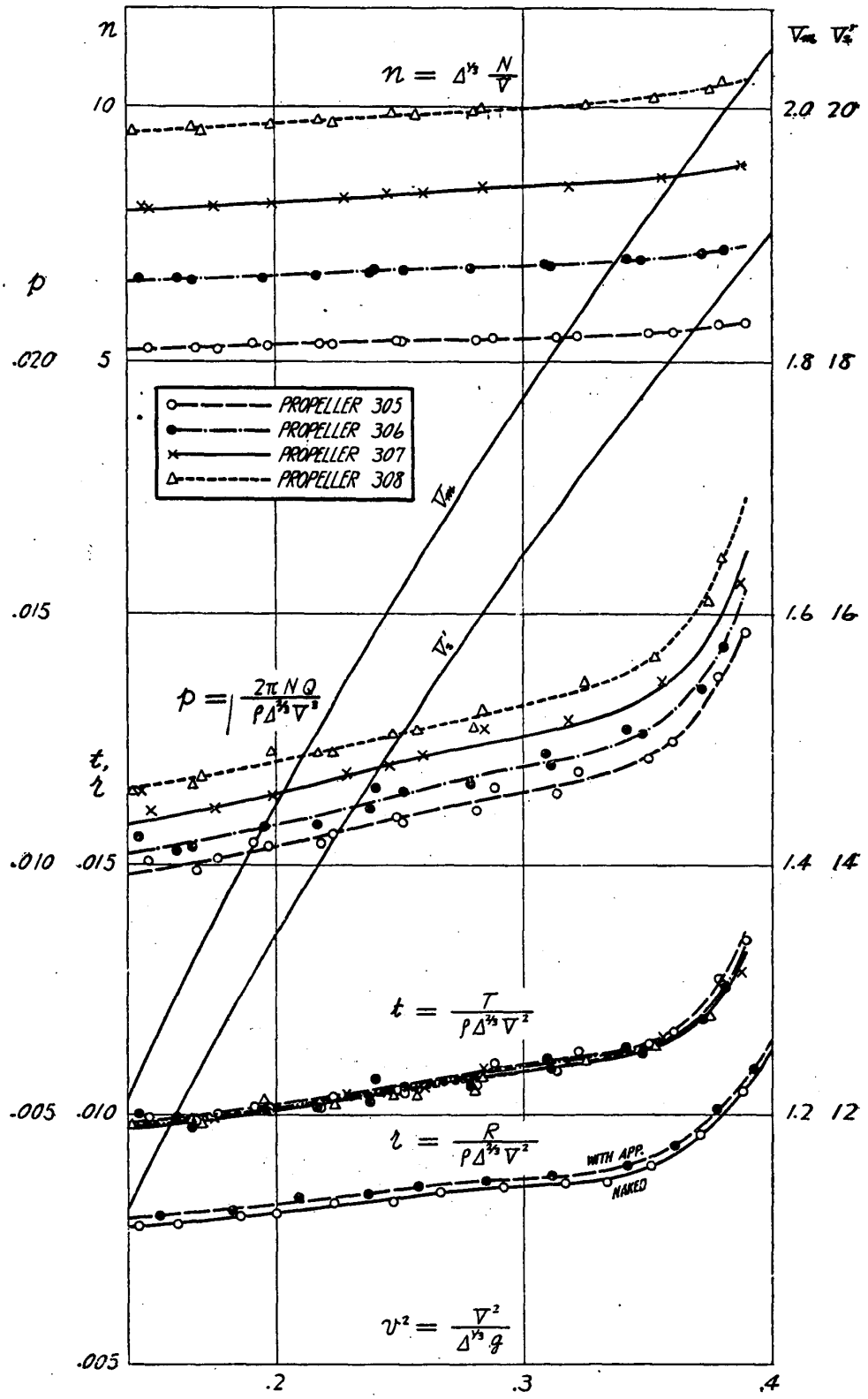

FIG. 34.—RESULTS OF SELF-PROPULSION TESTS OF MODEL 313.

NII-Electronic Library Service

The Society of Naval Architects of Japan

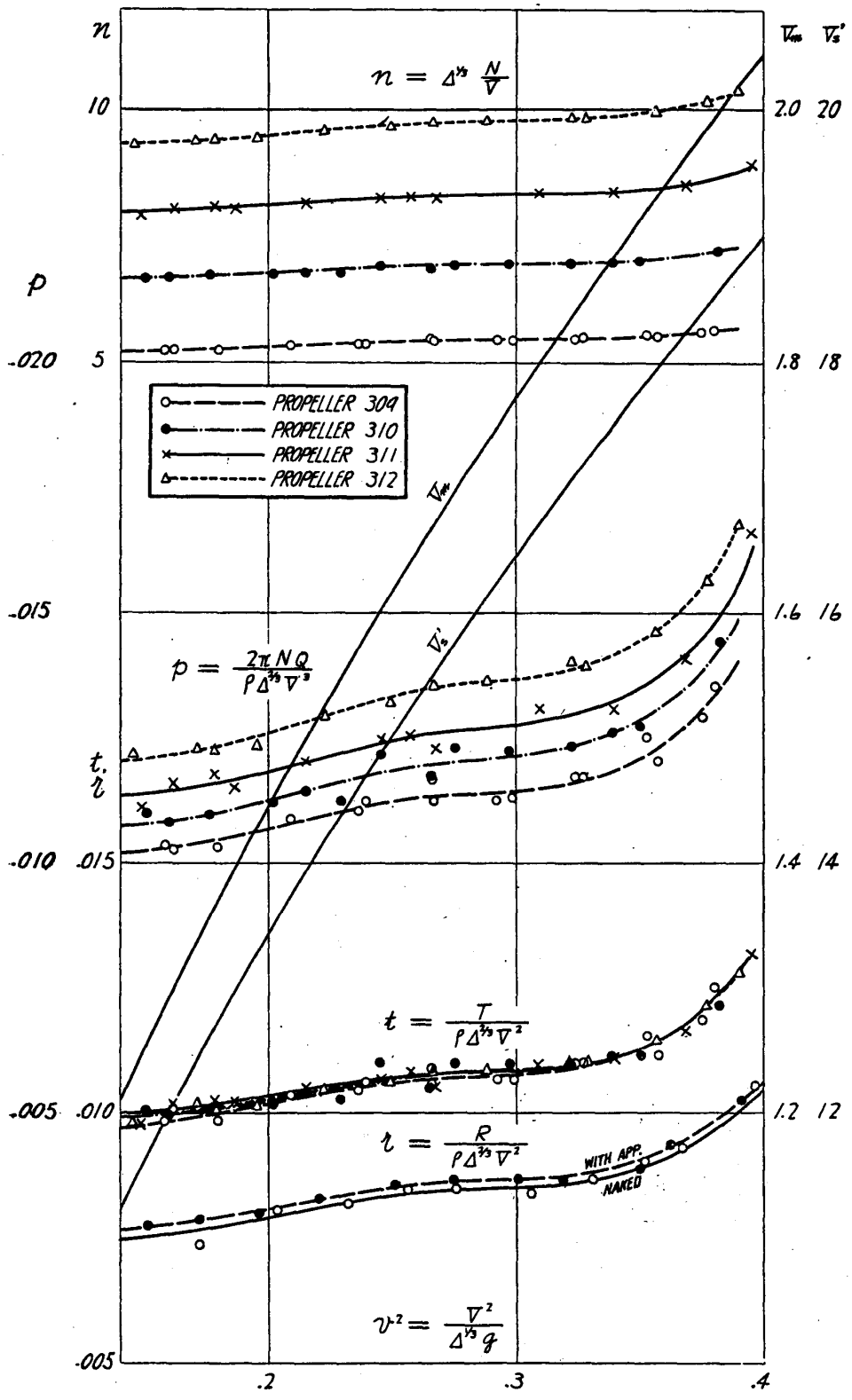

FIG. 35.—RESULTS OF SELF-PROPULSION TESTS OF MODEL 314.

NII-Electronic Library Service

The Society of Naval Architects of Japan

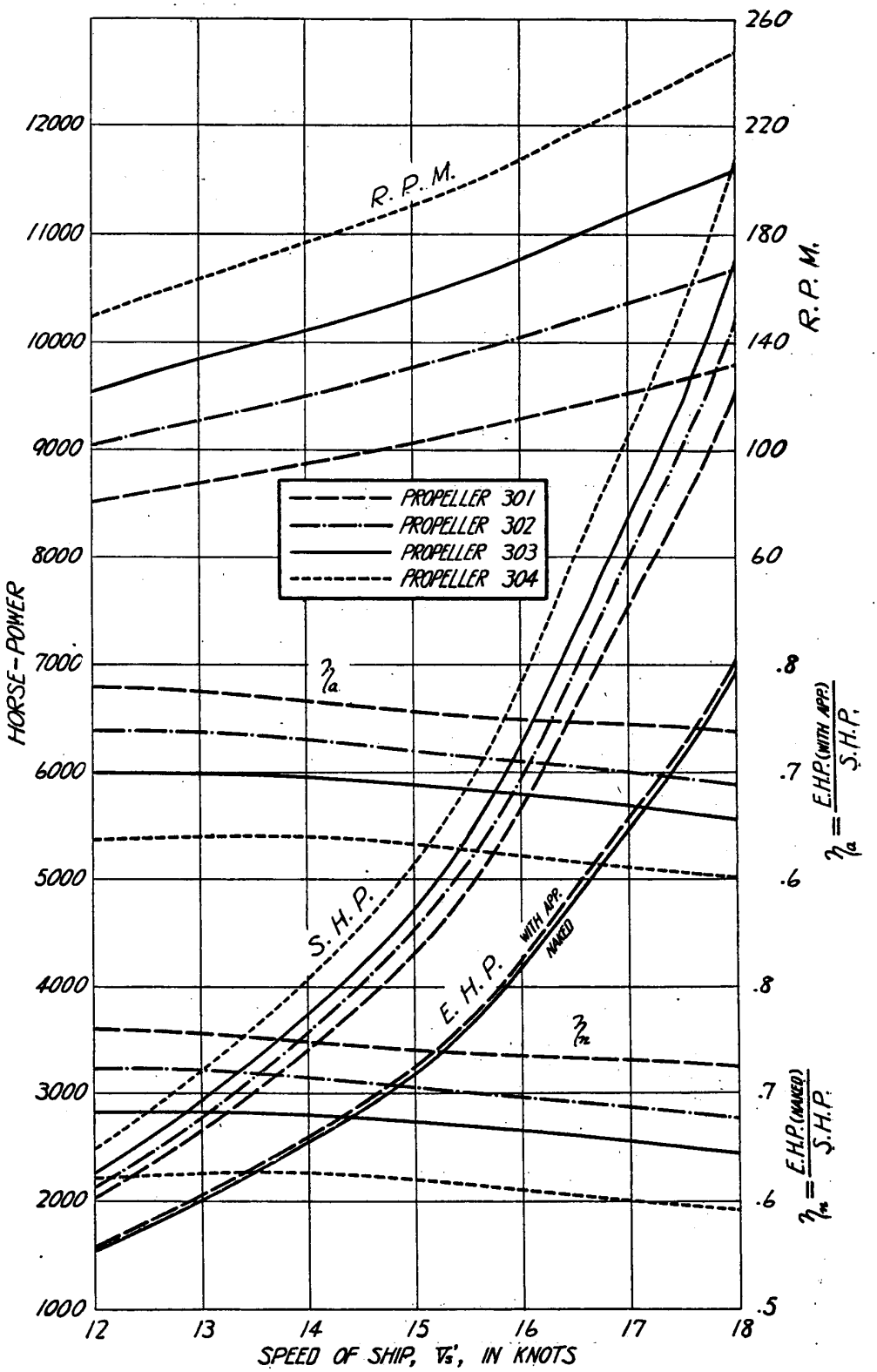

FIG. 36.—S.H.P., R.P.M., ETC. OF MODEL 312.

NII-Electronic Library Service

The Society of Naval Architects of Japan

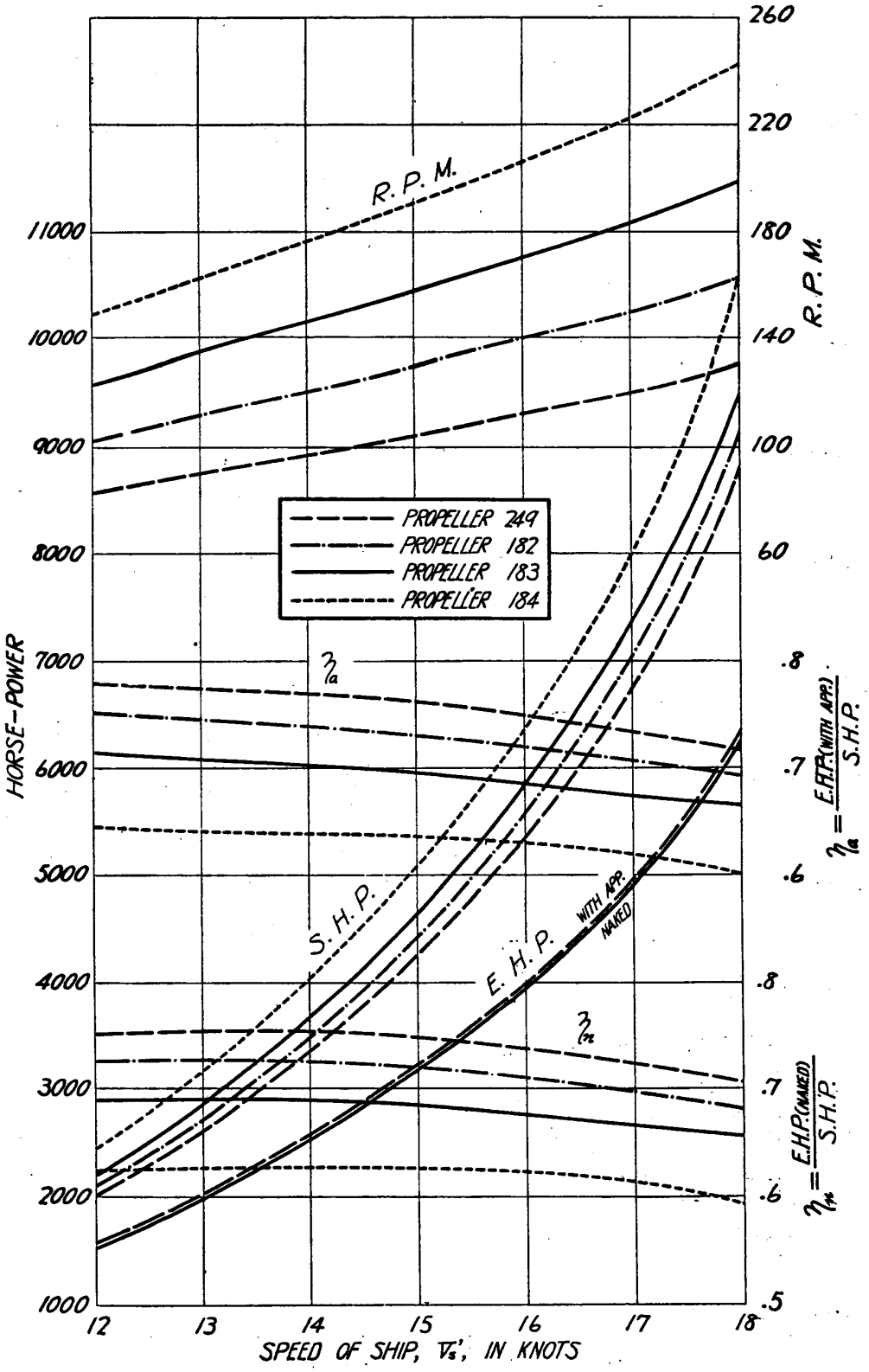

FIG. 37.—S.H.P., R.P.M., ETC. OF MODEL 237.

NII-Electronic Library Service

The Society of Naval Architects of Japan

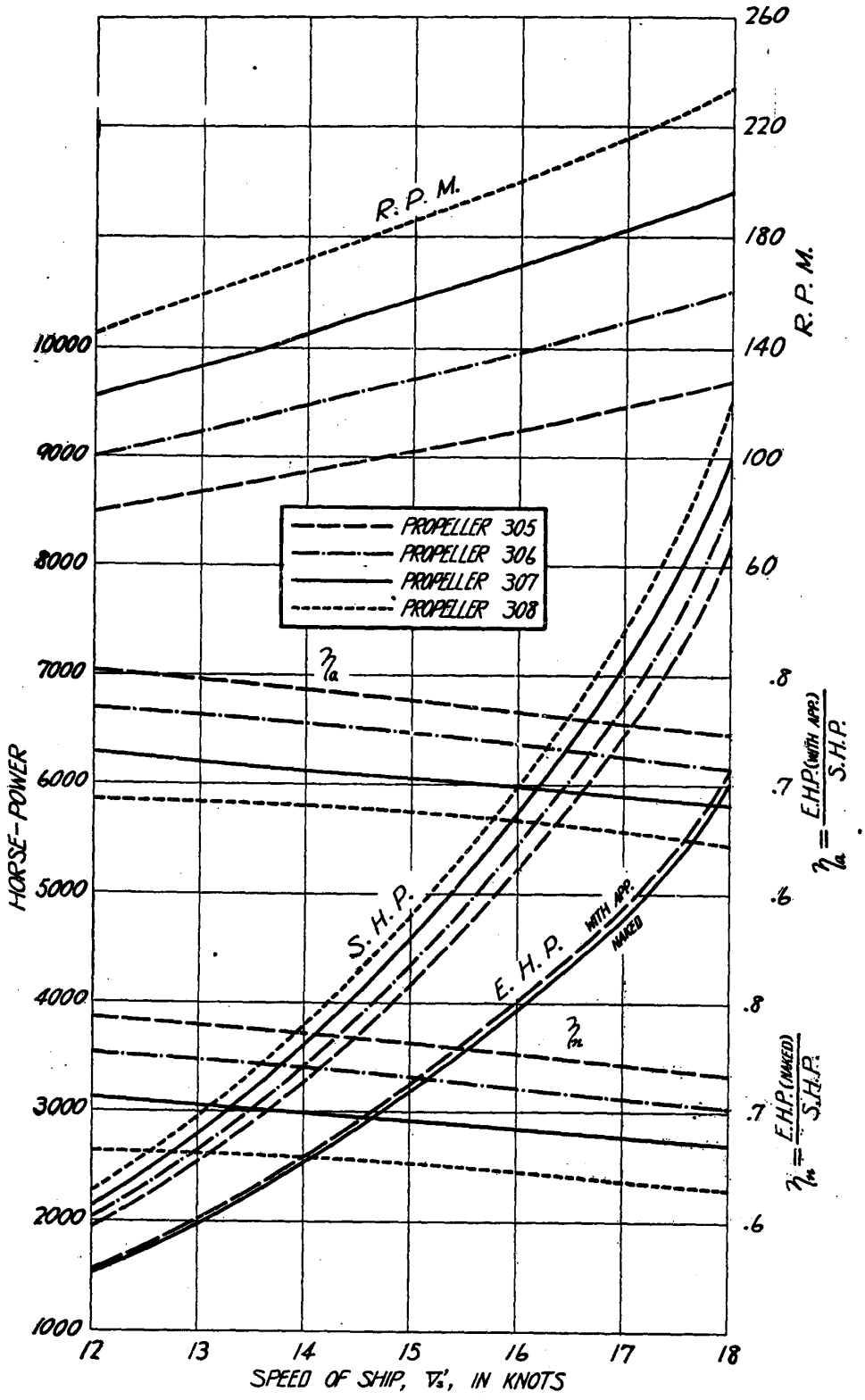

FIG. 38.—S.H.P., R.P.M., ETC. OF MODEL 313.

NII-Electronic Library Service

The Society of Naval Architects of Japan

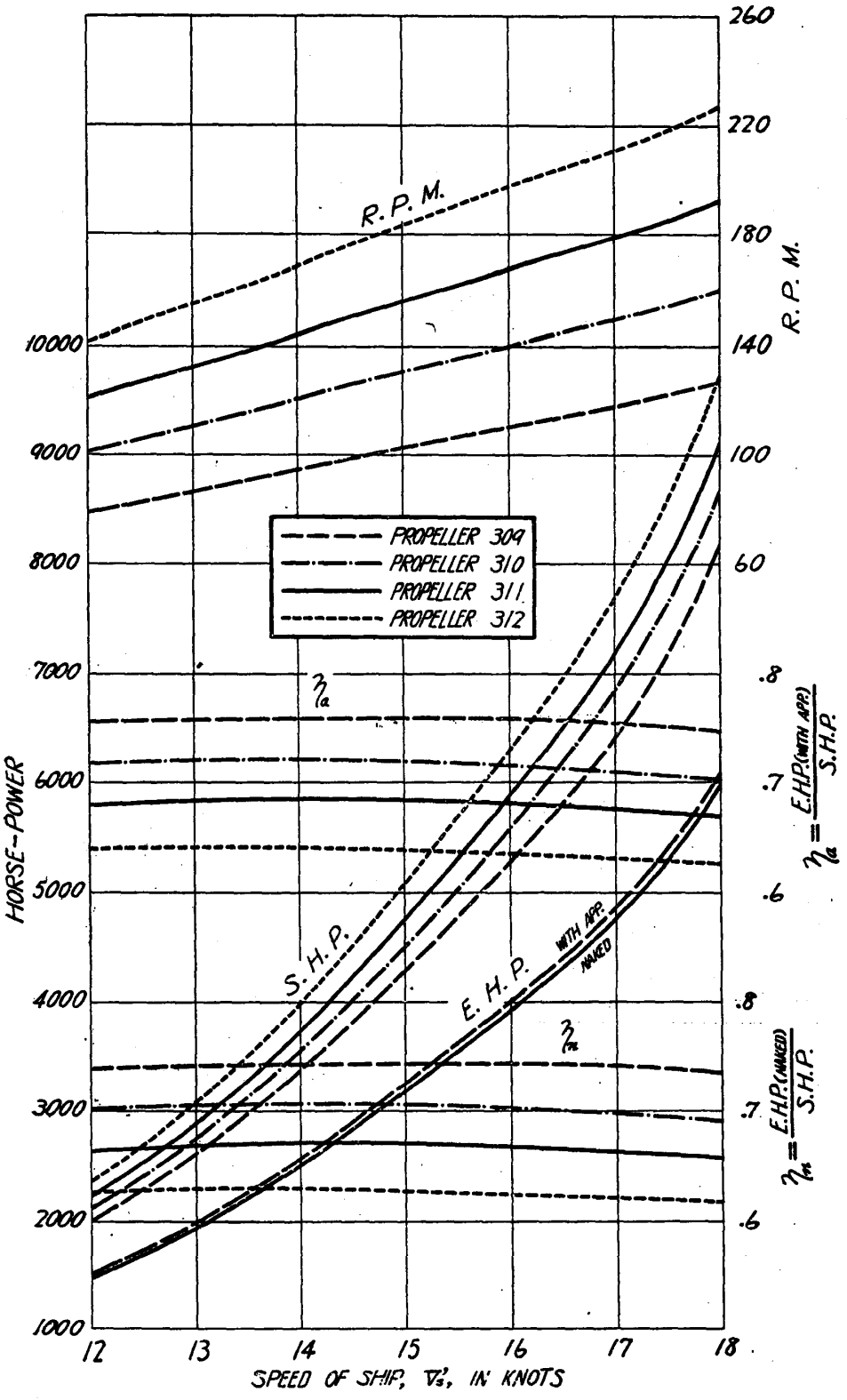

FIG. 39.—S.H.P., R.P.M., ETC. OF MODEL 314.

NII-Electronic Library Service

The Society of Naval Architects of Japan

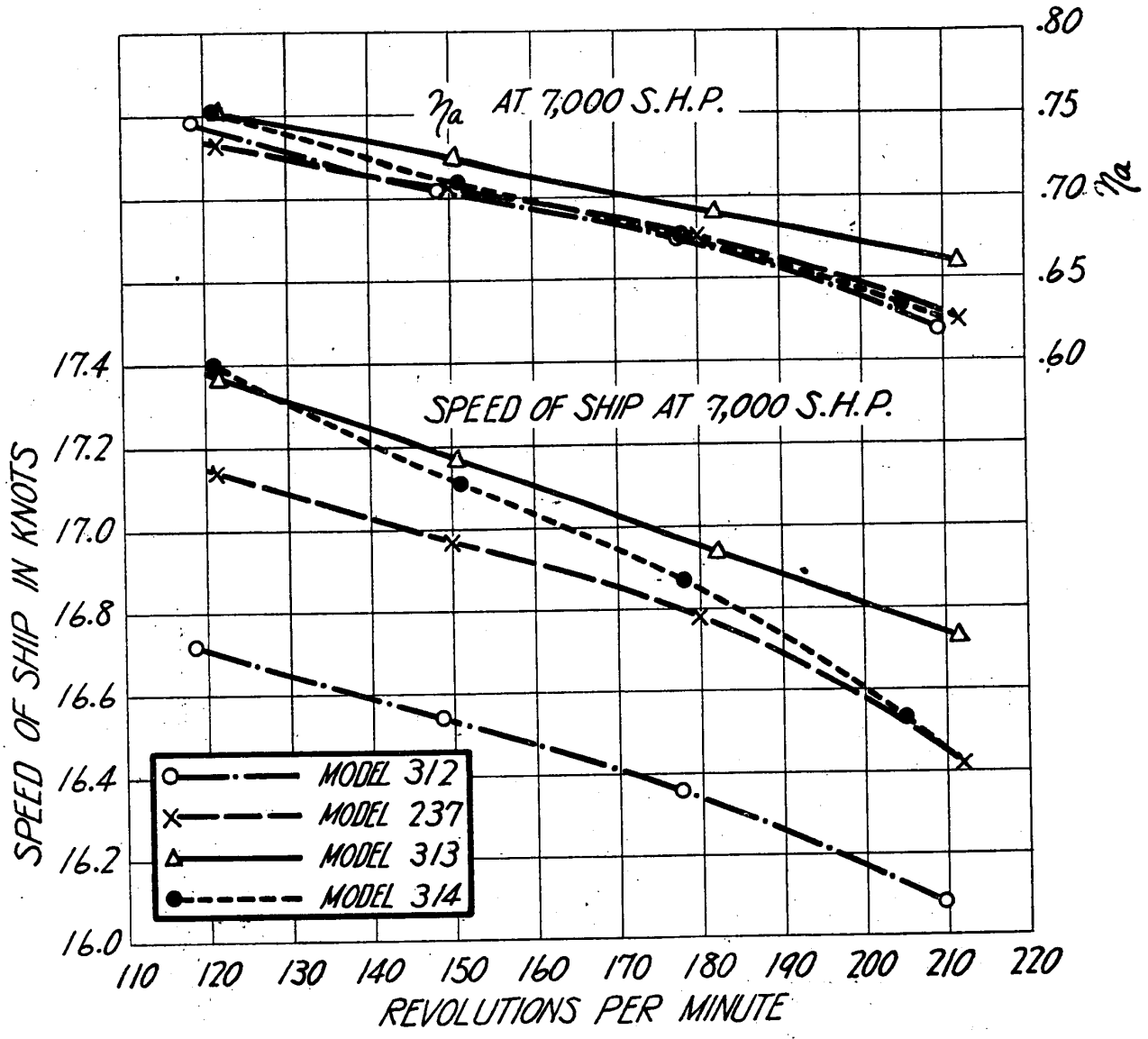

FIG. 40.—SPEED AND η_a AT 7,000 S.H.P.

NII-Electronic Library Service

The Society of Naval Architects of Japan

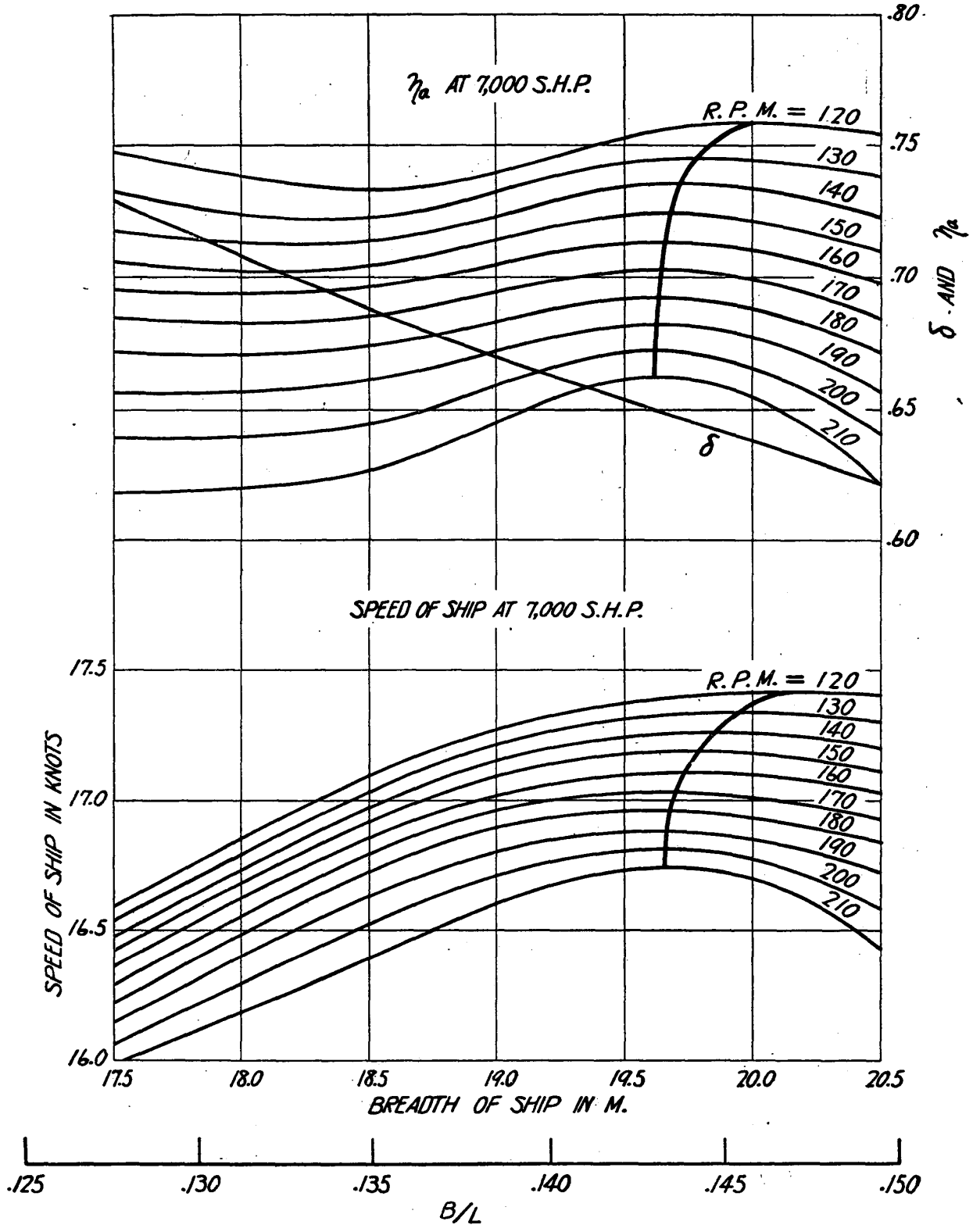

FIG. 41.—OPTIMUM BREADTHS AT 7,000 S.H.P.

NII-Electronic Library Service

The Society of Naval Architects of Japan

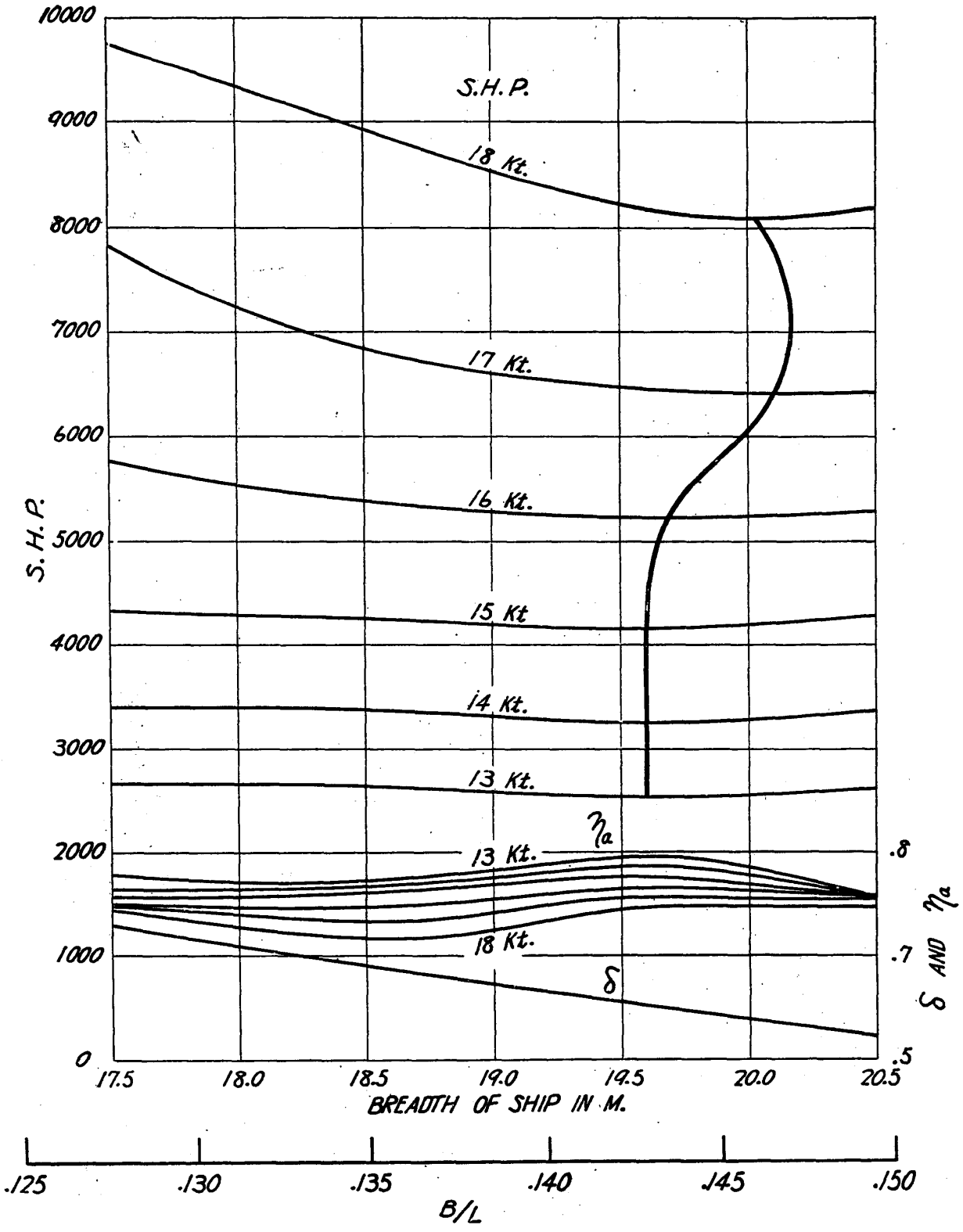

FIG. 42.—OPTIMUM BREADTHS (R.P.M. AT 7,000 S.H.P. =120).

NII-Electronic Library Service

The Society of Naval Architects of Japan

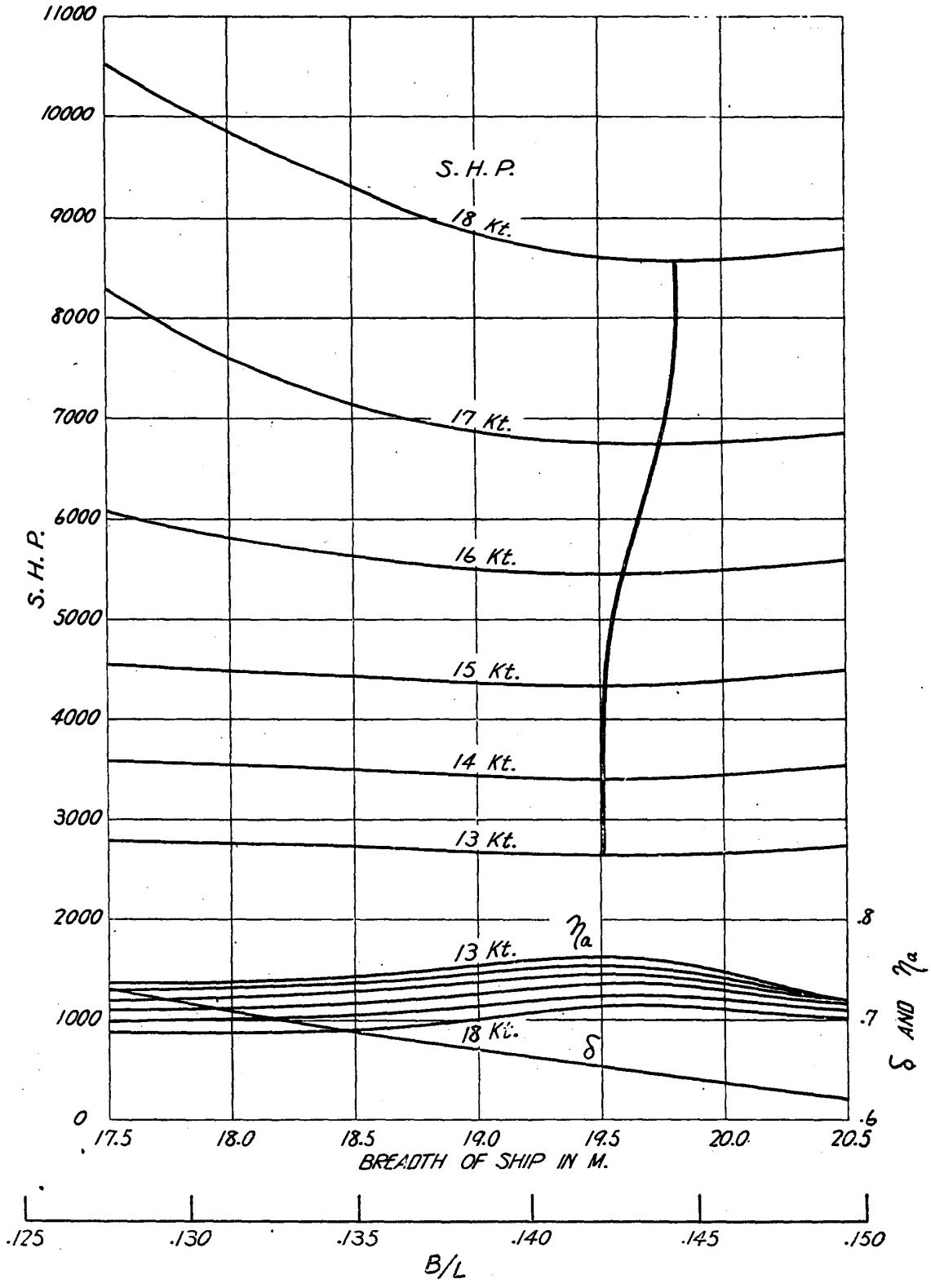

FIG. 43.—OPTIMUM BREADTHS (R.P.M. AT 7,000 S.H.P ≒ 15.0).

NII-Electronic Library Service

The Society of Naval Architects of Japan

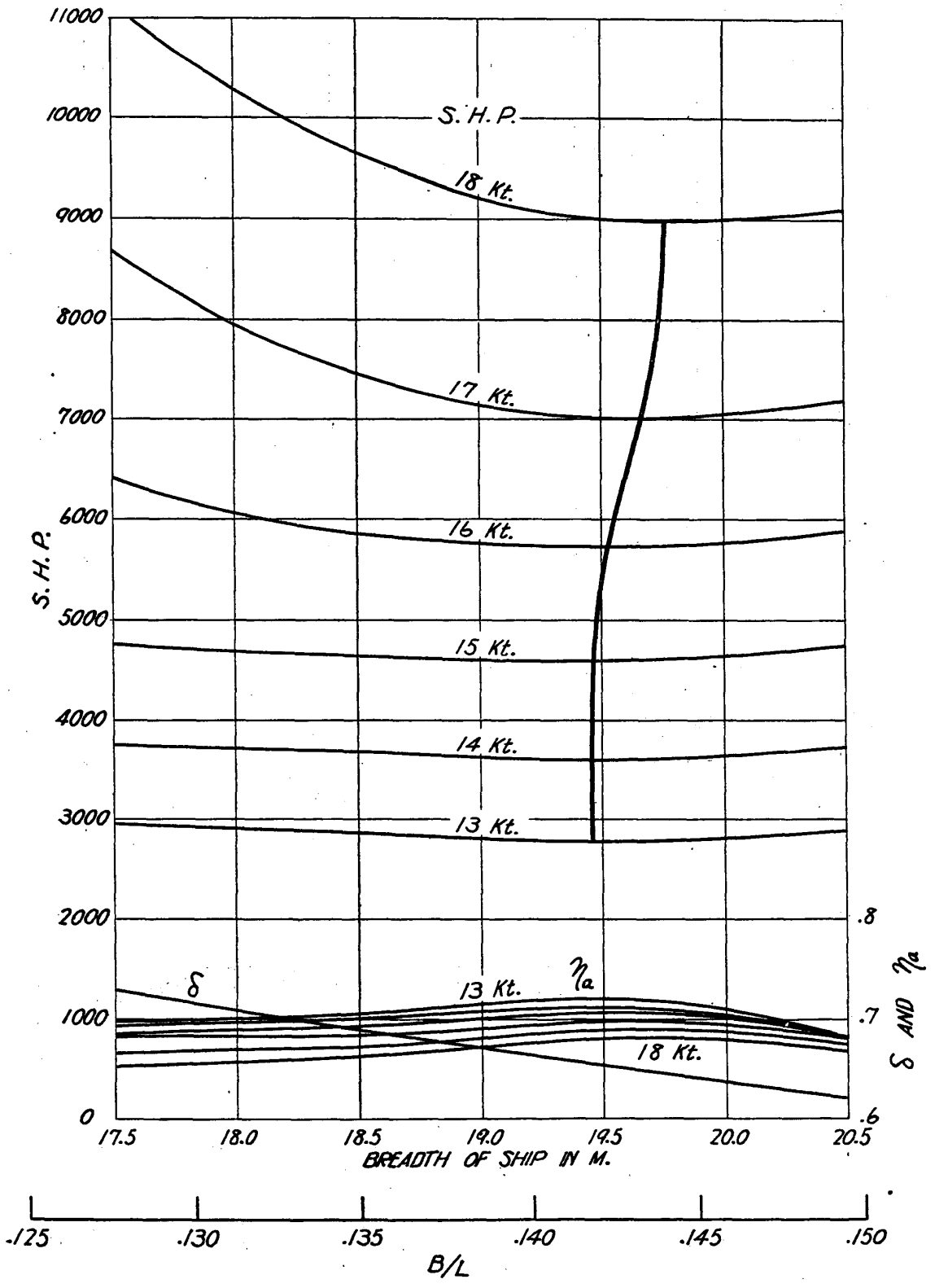

FIG. 44.— OPTIMUM BREADTHS (R.P.M. AT 7,000 S.H.P. ≒ 180).

NII-Electronic Library Service

The Society of Naval Architects of Japan

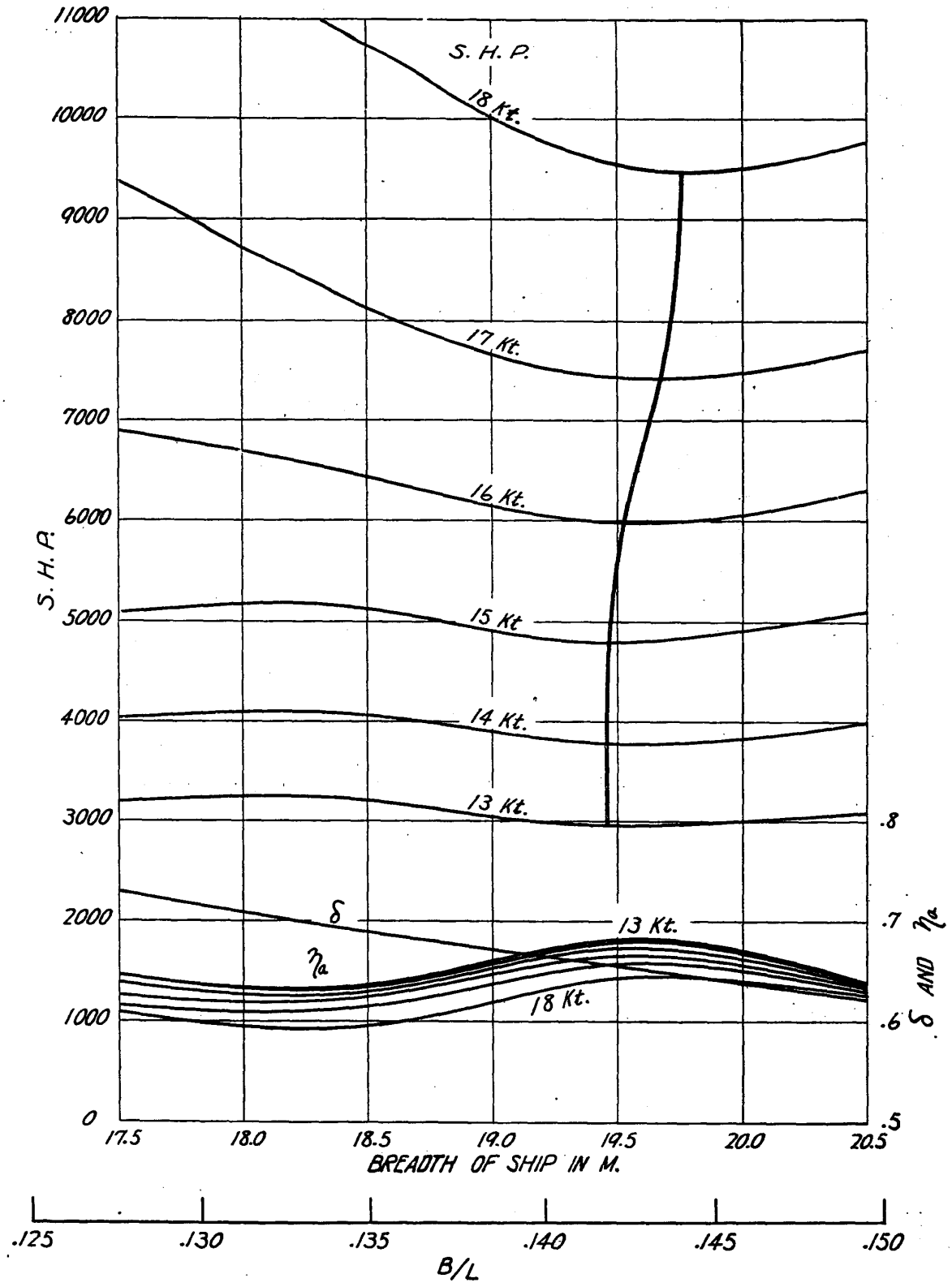

FIG. 45.—OPTIMUM BREADTHS (R.P.M. AT 7,000 S.H.P. ≒ 210).

NII-Electronic Library Service

The Society of Naval Architects of Japan

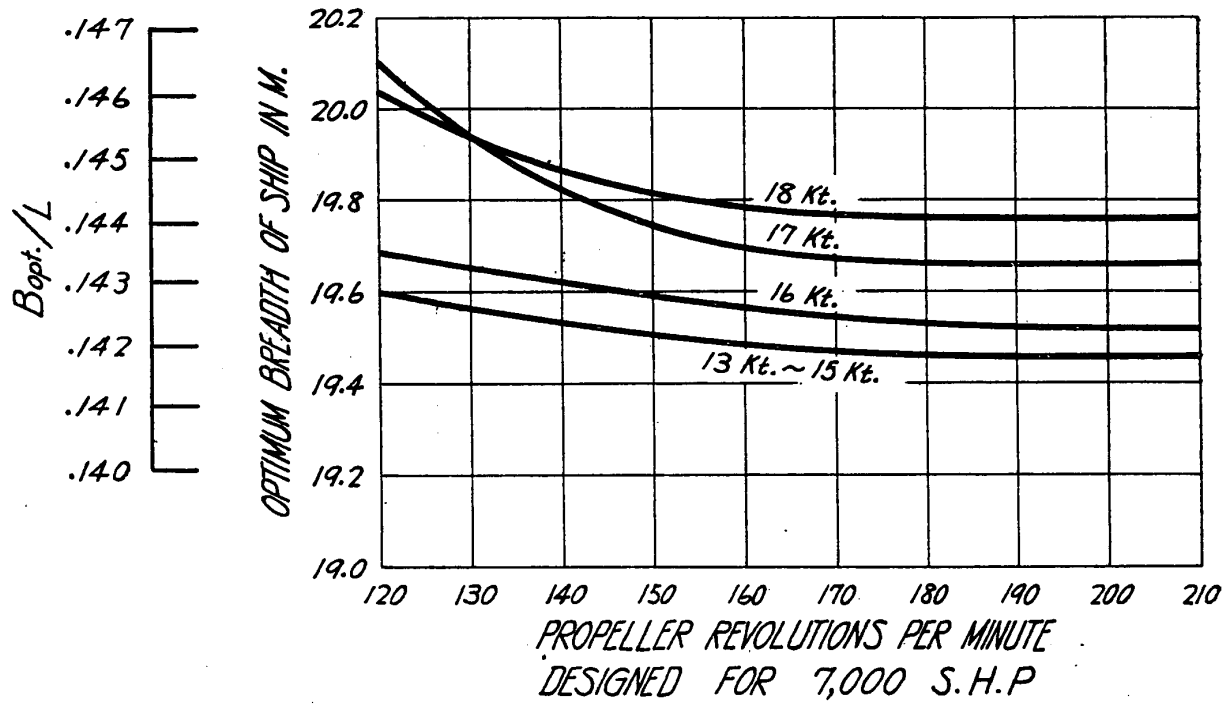

FIG. 46.— OPTIMUM BREADTHS AT VARIOUS SPEEDS.

NII-Electronic Library Service

The Society of Naval Architects of Japan

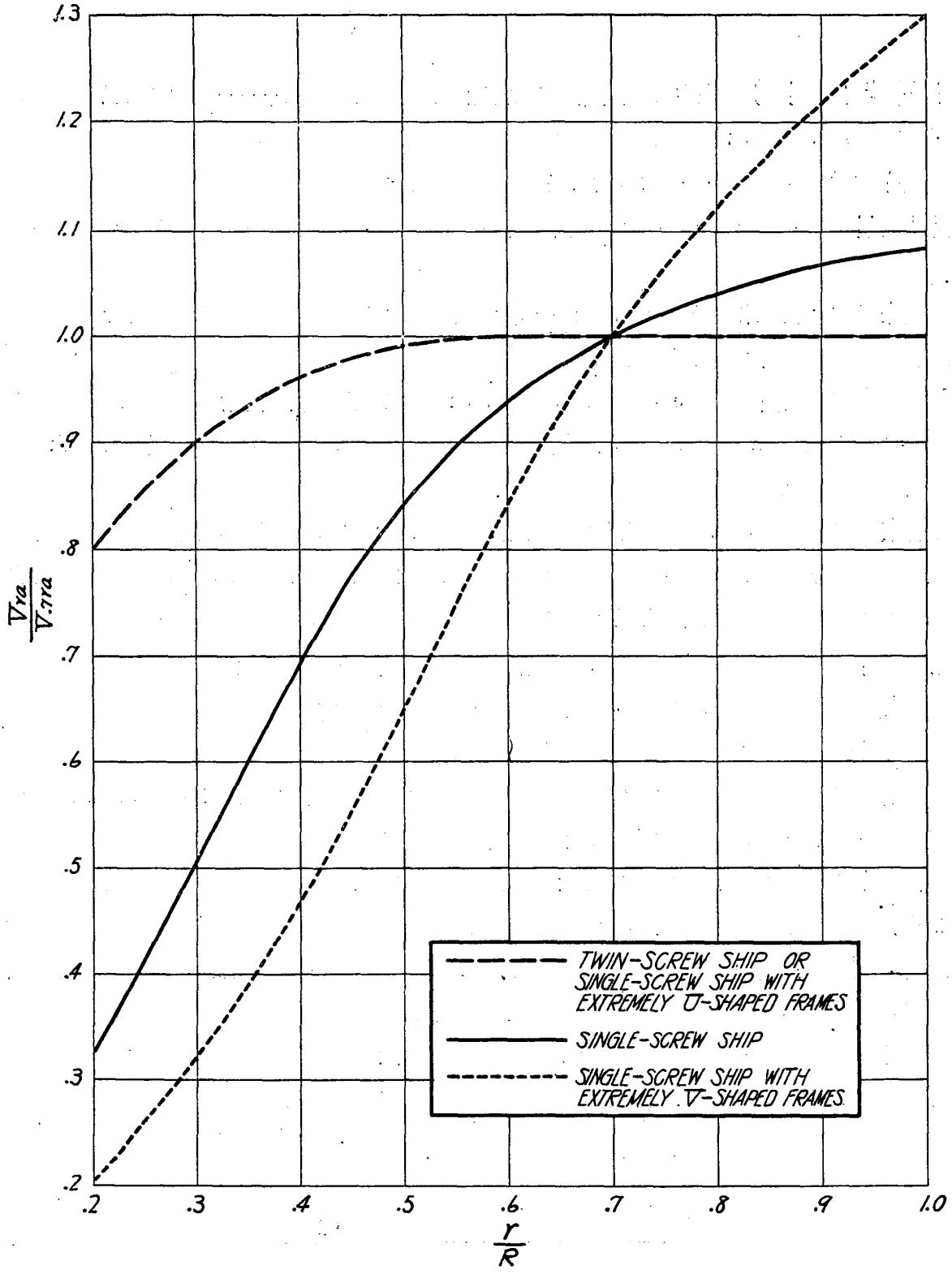

FIG. 47.—ASSUMED WAKE DISTRIBUTIONS.

NII-Electronic Library Service

The Society of Naval Architects of Japan

討　　論

○座長(平賀　讓君)　誰方でも御質問又は御意見がありますれば……無ければ私から、B/L とありますが L が constant ではないですか。

○山縣昌夫君　L が幾分違つても當て嵌まると思ひますが。

○平賀　讓君　air resistance は眞正面の場合ですか、斜からだと幅の effect が大きいと思ひます。

○山縣昌夫君　私は未だ air resistance の實驗をしたことが無いので良く判りませんが、此の場合は正面だけしか取扱つては居りません。

○出淵　巽君　最後の wake を estimate する curve ですが、私は商船の propeller のことは餘り良く存じませんが、immersion に相當變化がありますが、此の immersion に因つて wake が變化することはありませんか。

○山縣昌夫君　此の curve は主として貨物船に就いて full load ばかりの狀態で考慮したので特殊の船は入つて居りませぬ。cargo ship で 100 隻程の實驗結果の平均を示したものでありますから cargo ship では先づこれで良いと思ひます。

○平賀　讓君　先刻の B/L で length が增すと大いに變ると思ひますが。

○山縣昌夫君　B/L は similar の船に就いて言つてゐるのです。

○平賀　讓君　さうすると B/L ではなく B ではないですか。

○山縣昌夫君　B は 450 呎に對する B であつて、similar の船に就いても optimum line 等が略ゝ適用出來ると思つて B/L も掲げて置いたのであります。

○平賀　讓君　いや、私が考へ違ひを致して居るかも知れません。どうも有難うございます。

○山縣昌夫君　私が考へ違ひをしたのかも知れません。

○座長(平賀　讓君)　他にありませぬなら私から一言申上げます。山縣博士は多年に亙り何回となく resistance 及び propulsion に關する有益なる論文を發表され、本日のも亦其の中の一つであり、我が國の resistance & propulsion の研究に多大の貢献をせられたのであります。本日の有益なる論文に對して皆樣と拍手を以て御禮申上げたいと思ひます。(一同拍手)

NII-Electronic Library Service